universität wien

DIPLOMARBEIT

Titel der Diplomarbeit

"hsa-miRNA-663 in replicative and DNA damage induced senescence of human dermal fibroblasts"

Verfasserin

Kathrin Ingrid Garschall

angestrebter akademischer Grad

Magistra der Naturwissenschaften (Mag.rer.nat.)

Wien, 2013

Studienkennzahl lt. Studienblatt:	A490
Studienrichtung lt. Studienblatt:	Molekulare Biologie
Betreuerin / Betreuer:	Univ.-Prof. Dr. Andrea Barta

CONTENTS

1 ABSTRACT

Aging is a multifactorial and highly regulated process that starts on cellular level and finally affects the whole individual with tissue deterioration, leading to disease and an increased probability of death with the progression of lifetime. Based on the findings, that hsa-miRNA-663 is upregulated in the cellular senescence of human diploid fibroblasts (HDF), we aimed to further elucidate the role of this small non coding RNA, which was recently shown to act as tumor promoter or suppressor dependent on cancer cell type. A bioinformatical target prediction matched its seed region to the cell cycle phosphatase PP5, a ubiquitous protein that interferes with multiple pathways of proliferation, DNA damage and apoptosis signaling. PP5 also participates in the regulation of the cellular stress mediator p53 that – amongst many other functions - can induce transcription of p21 (cyclin-dependent kinase inhibitor 1) to promote a cell cycle arrest in G1 phase.

Although we could not verify a direct interaction between miR-663 and PP5 using a dual luciferase reporter system, we found that transient induction of miR-663 correlates with reduced abundance of PP5 protein yet not with a consistent reduction of PP5 mRNA. We found that induction of miR-663 and siRNA mediated knockdown of PP5 both reduced the levels of p21 mRNA but had no effect on the proliferative potential, assayed by BrdU incorporation. Finally were able to show an increase in p21 mRNA upon treatment of HDF with sublethal doses of hydrogen peroxide, which did not correlate with the levels of miRNA-663 or PP5 mRNA.

2 INTRODUCTION

2.1 Aging and senescence

Aging is a biological phenomenon that is commonly characterized by a progressive functional decline which ultimately leads to death. Although it is a fundamental and - so far - inevitable concomitant to human life, not many of the underlying processes and mechanisms are well understood yet.

There are many theories on the causes of aging. Some see these in the gathering of damage over the time that leads to cellular and then tissue and finally organ malfunctions that cannot be repaired anymore (the damage/maintenance paradigm). Others hold processes responsible, that had been important for development and growth earlier in life (hyperfunction theory), but whose deregulation with advanced age leads to pathologies and terminally to death - as recently reviewed (Gems and Partridge, 2012)

It is well-accepted though, that aging is a multifactorial process and the result of the sum of endogenous and exogenous influences from individual cells to organismal level. Pathways that were shown to be important for aging, deal with signals on cellular stress level, genome integrity and metabolic status. The regulatory network that deals with sensing of nutrients (Insulin/IGF-1 and TOR signaling, as well as the AMP kinase pathway) plays a distinctive role for aging and the onset of senescence. In animal models remarkable changes in lifespan could be achieved by interfering with these pathways (Kenyon, 2005, 2010)**.**

2.1.1 Replicative senescence

When Hayflick and Moorhead, 1961, transferred primary cells from human tissue to culture medium and found a limit to cell proliferation, they revised the dogma of cell immortality and stated that aging might already happen on cellular level (Hayflick, 1965). The loss of long term proliferative capacity in somatic cells despite their metabolic activity, was attributed to the DNA loss that occurs in each cell division – the “end replication problem”: On every round of DNA replication, a fraction of the telomeres – protective non coding sequences at the end of each chromosome – are not copied and leave the newly synthesized chromosomes shorter than the original ones, restricting replication potential (Watson, 1972).

At a certain threshold of telomere length a DNA damage response (DDR) is induced (Fagagna et al., 2003), accompanied by epigenetic responses (such as introduction of phosphorylated histone variant γ-H2AX), expression of certain proteins (such as 53BP1, NBS1, MDC1) and activation of DNA damage kinases ATM and ATR. As a consequence, the cell cycle is arrested for DNA repair. In case the damage

cannot be repaired, pathways are activated that either promote programmed cell death (apoptosis) or replicative senescence (RS) (Fagagna, 2008).

If, however, the cells escape this growth arrest and proliferate further, they reach a state called crisis, where the continuous loss of valuable genetic information with every replication results in chromosome instability and normally cell death (Shay and Wright, 2005).

Somatic cells that gain the potential to rebuild their lost telomeres are a danger to the human organism and prerequisite for cancer. They exceed their telomere determined proliferation limit and become immortalized, either by activation of telomerase (an enzyme that binds to chromosome ends and adds the typical repetitive sequences) or by using telomeric DNA from other chromosomes to recombine with the damaged ends (ALT: Alternative lengthening of telomeres) (Colgin and Reddel, 1999; Henson et al., 2002)**.** Consequently cellular senescence is considered an important mechanism to prevent cancer development (Campisi, 2005).

2.1.2 Premature cellular senescence

Independent of telomere length, DNA damaging agents and genetic aberrations can induce a persistent cell cycle arrest. Hydrogen peroxide treatment for instance imposes oxidative stress on the cells and leads to a senescence like growth arrest in human fibroblasts (Chen and Ames, 1994). Also the activation of certain oncogenes or the loss of tumor suppressor genes can induce a state of premature senescence, preventing a progression to malignant transformation (Mallette and Ferbeyre, 2007).

2.1.3 Paths to senescence

As mentioned above, the complex multi-pathway system ultimately leading to cellular senescence features a tight web of feedback regulations from all aspects of cellular life, of which many are not yet fully uncovered.

While the signals transmitting information about potentially oncogenic stimuli (such as telomere shortening, DNA damage or activation of tumorigenic factors) are diverse and often specific to the cause, their cumulated effect – a stable cell cycle arrest – is strongly dependent on the upregulation of inhibitors for cell cycle progression, such as $p21^{WAF1}$ (CDKN1A) and $p16^{INK4}$ (CDKN2A) summarized in **Figure 1** (Alcorta et al., 1996; Stein et al., 1999).

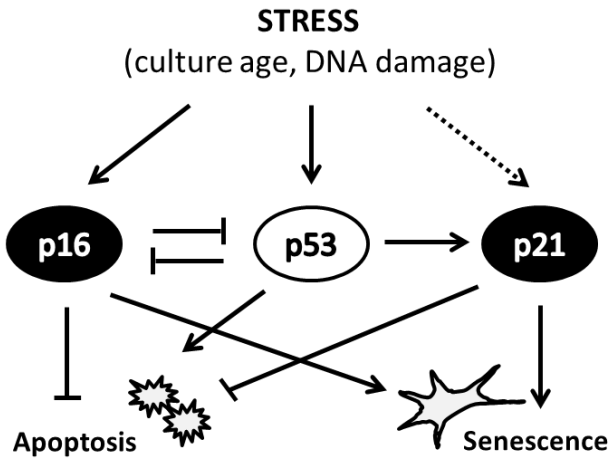

Figure 1: Cartoon overview on the role of tumor suppressors p16, p53 and p21 in senescence of human fibroblasts **(Mirzayans et al., 2012)**, slightly modified: Telomere shortening or exposure to DNA damaging agents activates p53 which induces senescence via p21 or apoptosis (dependent on the degree of DDR) and represses p16. Upregulation of p16 inhibits apoptosis and induces senescence.

p16 expression is induced by several stress and tumor signaling pathways (Jacobs and Lange, 2005), inhibits the activity of several cyclin dependent kinases to block cell cycle transition from G1 to S-phase and induces transcriptional silencing of positive cell cycle regulators, recently reviewed by (Mirzayans et al., 2012).

One of the main cellular stress mediators is p53, which is a common target of numerous signaling cascades and modified dependent on the source of damage in the cell. In response to DNA damage, p53 is stabilized by certain phosphorylations and can enter the nucleus to activate transcription of genes which improve cellular and genetic stability (review by (Efeyan and Serrano, 2007)

p21 is one of the downstream effectors of activated p53 and has been associated with an age related cell cycle arrest following double strand breaks (DSBs) due to telomere shortening or due to DNA damaging agents (e.g. UV-radiation). When it localizes to the nucleus, p21 participates in the establishment of cellular senescence (Romanov et al., 2012).

2.2 Micro RNAs

Micro RNAs (miRNAs) are short (~21-23bp), endogenous non-coding RNA molecules that regulate gene expression by targeting mRNA in their untranslated regions (UTR).They regulate numerous pathways and are usually generated from characteristic hairpin structures in RNA polymerase II transcripts, that are cleaved by the Microprocessor complex (RNase DROSHA and DGCR8) or that are products of mRNA splicing events (Bartel, 2004; Berezikov et al., 2007; Gregory et al., 2006).

After active export from the nucleus into the cytoplasm, they are further cleaved by Dicer and the so called guide-strand is incorporated into the RNA induced silencing complex (RISC) (see **Figure 2**). One of the miRNA strands serves as a matrix to find mRNAs via pairing with the miRNA seed region (typically a 6-8mer of bases). The fact that miRNAs do not need total complementarity enables them to regulate multiple mRNAs that match their seed region, but adds complexity to bioinformatical

target prediction. Upon binding of the miRNA-RISC (miRISC) to an mRNA it either accelerates its degradation (via deadenylation of the Poly(A) tail and decapping) or interferes with translation, leading to mRNA accumulation in so called P-bodies (Eulalio et al., 2008; Fabian and Sonenberg, 2012; Rana, 2007).

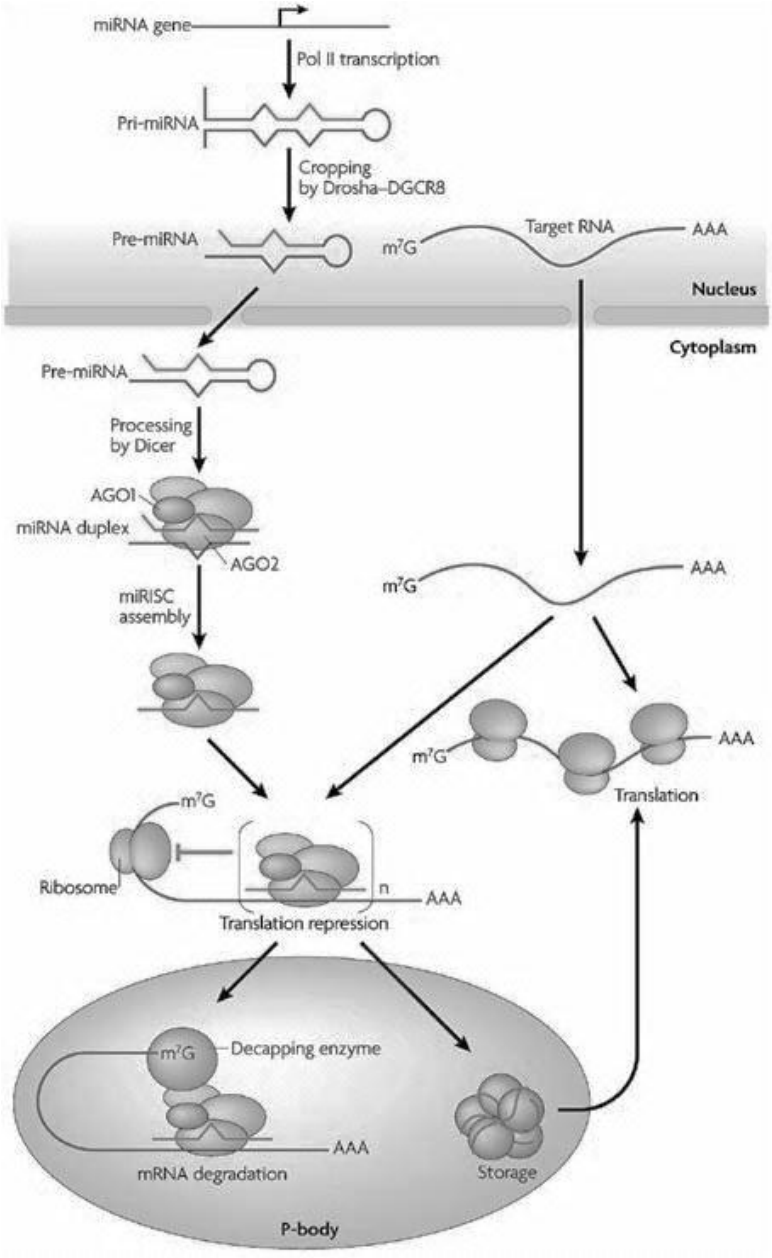

Figure 2: Model for human miRNA- RISC function (Rana, 2007): MicroRNA genes are transcribed by RNA polymerase II and cleaved by the Drosha–DGCR8 complex. After transport to the cytoplasm, Dicer processes them into mature miRNAs that assemble into the RNA-induced silencing complex (RISC). Several RISC loaded with miRNA (miRISC) bind to target mRNA and induce cleavage or accumulation in P-bodies for storage.

2.2.1 miRNAs in aging and senescence

As one microRNA can target multiple mRNAs and - on the other hand - a single mRNA can be targeted by multiple miRNAs (Krek et al., 2005), it is not surprising that they also play an important part in the multi-layered regulation of aging. In fact, lin-4, one of the first miRNAs described (Lee et al., 1993) and discovered in the nematode *Caenorhabditis elegans* (*C. elegans*), was found to increase lifespan upon overexpression (Boehm and Slack, 2005). Since then, many more miRNAs have been characterized in pathways for proliferation, oncogene repression and senescence and they seem to play an important role: one general trend in aging is a decrease in miRNA abundance; miRNA biogenesis mutants in the fruitfly *Drosophila melanogaster* and *C. elegans* show a clear decrease in lifespan and Dicer knock down induces senescence in mice (Kato et al., 2011; Liu et al., 2012; Mudhasani et al., 2008).

A recent review by (Smith-Vikos and Slack, 2012) summarizes the interference of miRNAs with aging pathways that are known so far (see **Figure 3**): mitogen induced senescence is accompanied by a decrease of several miRNAs (Marasa et al., 2009), 25 miRNAs were found to be differentially expressed upon oxidative stress induced senescence (Li et al., 2009), p53 is regulated by and promotes upregulation of miRNAs (Ugalde et al., 2011; Yamakuchi and Lowenstein, 2009) and a whole cluster of miRNAs that influence insulin signaling is downregulated in human aging (Grillari et al., 2010)**.**

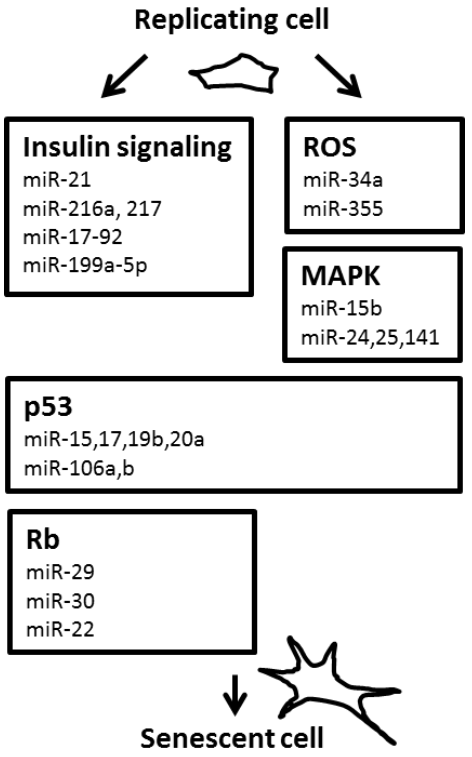

Figure 3 miRNAs in aging **(Smith-Vikos and Slack, 2012)**; modified. miRNAs regulate gene expression of components of aging pathways (outlined in boxes) on the cellular level: They interfere with insulin signaling representing metabolic status, regulate stress responses to reactive oxygen species (ROS) or mitogen activation (MAPK pathway) and modify p53 and Rb mediated proliferation (stop) signals.

2.3 PUVA treatment and skin aging

This work bases on the findings by Harald Kühnel (unpublished), who performed a microarray analysis of miRNA genes in primary human diploid fibroblasts (HDF) of young and old donors as well as from HDF that had undergone a combinational treatment of psoralens and long wave UV-A radiation (PUVA).

This photochemical treatment is used to treat severe immune-mediated skin disorders (such as psoriasis, vitiligo, atopic dermatitis) and relies on the fact that psoralens intercalate with the DNA and form interstrand crosslinks upon photo-activation (Cimino et al., 1985; Morison, 1999).

These crosslinks block DNA replication and lead to a p53 dependent DNA damage response which can lead to apoptosis of treated cells (Derheimer et al., 2009; Mogi et al., 2008). A side effect of long term PUVA treatment is premature aging of the treated cells. (Wlaschek et al., 2003)

To investigate microRNA regulations in senescence, Harald Kühnel et al. compared the expression profiles of HDFs in replicative senescence and after PUVA treatment (Hovest et al., 2006), to those of young and UV-A treated cells on a micro-array. Amongst many differentially regulated miRNAs (unpublished), they saw a shared upregulation in the expression of an – at that time - uncharacterized miRNA (hsa-miR-663) in the cells with senescent phenotype.

2.3.1 Hsa-miR-663

MiRNA-663 is transcribed from human chromosome 20: 26,186,822-26,190,914 and its mature form is the minus strand sequence: 3'-AG**GCGGGG**CGCCGCGGGACCGC-5'(seed region for target specificity highlighted by box) according to miRBase.com (Griffiths-Jones et al., 2008).

In the meanwhile hsa-miR-663 expression was associated with the regulation of various pathways in cancer, where it seems to function – dependent on cell type – either as a tumor suppressor or promoter:

In gastric cancer, miRNA-663 is downregulated while its overexpression causes growth suppression of cells in vitro and in vivo (mouse xenograft) shown by (Pan et al., 2010)**.** Treatment of colorectal cancer cells with Resveratrol stimulates miR-663 expression, reducing TGFβ signalling (which can be either inhibiting or promoting tumor progression)(Tili et al., 2010a) and for human leukemia cells it was shown, that miR-663 was highly expressed following all trans retinoid acid (ATRA) treatment and that it is sufficient to induce differentiation and growth arrest (Pan et al., 2011).

In lung cancer and nasopharyngeal carcinoma cells (NPC) miR-663 acts as an oncogenic miRNA by supporting aberrant cell cycle transition and promoting proliferation. Inhibition of miR-663 in these cells led to an upregulation of tumor suppressor genes and in vivo inhibition on grafted NPC slowed their growth. (Liu et al., 2011; Yi et al., 2012)

Hsa-miR-663 has also been of interest to the aging research: it was found to be upregulated in screening experiments on replicative senescence, quiescence and DNA damage induced senescence in human diploid fibroblasts (HDF) and correlated with Id1 (leading to activation of p16) and insulin like growth factor receptor 1 downregulation (Maes et al., 2009; Marasa et al., 2010)**.** However, a clear functional characterization of miR-663 in senescence of HDF has not been published yet.

We performed a bioinformatical target search using microCosm[1] software and found three possible binding sites of miR-663 in the 3' UTR of cell cycle phosphatase PP5 (Protein Phosphatase 5) mRNA.

2.3.2 Protein Phosphatase PP5

PP5 has been implicated in a wide area of modifying cellular signaling, amongst others, pathways for proliferation, apoptosis and DNA damage repair: it plays a major role in the inactivation of MAPK signaling, removes phosphorylation from p53 binding Protein 1 and counteracts the checkpoint kinases ATM and ATR – making it an interesting candidate in aging research (Hinds Jr. and Sánchez, 2008).

In our working hypothesis (**Figure 4**), miRNA-663 upregulation in senescence leads to a reduced abundance of PP5 and consequently to an increase of phosphorylated p53 (and other signal transducers as the result of DNA damage and cellular stress). With aging these signaling factors surpass a certain threshold, and a p21 dependent growth arrest is established to induce the necessary repair mechanisms. We hypothesized, that miR-663 expression is kept high in senescence to stabilize the cell cycle arrest in HDFs.

[1] http://www.ebi.ac.uk/enright-srv/microcosm/htdocs/targets/v5/info.html#

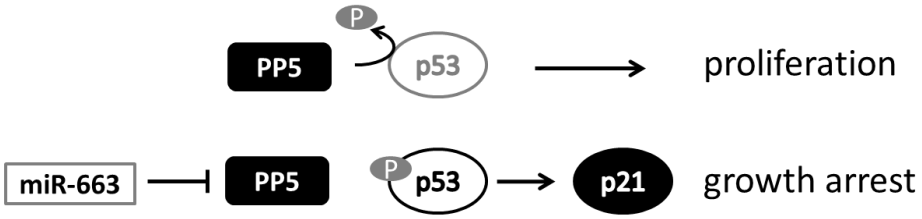

Figure 4 Depiction of our working hypothesis on miRNA-663 and PP5 in cellular senescence. Under normal conditions, PP5 keeps signaling p53 dependent transcription at a basal level by removing stabilizing phosphorylations from p53. With age, the cellular level of activated p53 (and other stress signal transducers) rises and miRNA-663 is expressed to lower the abundance of PP5. This leads to a further increase of phosphorylated p53 and transcription of the dependent response genes: amongst them p21, which then can induce a G1 growth arrest.

2.4 Objectives

To elucidate the correlations between miRNA-663 and PP5, we overexpressed miRNA-663 in young, replicating primary HDFs and determined the effect on PP5 mRNA and protein levels. We also assessed miRNA-663 expression under DNA damage conditions by exposing the cells to sublethal doses of H_2O_2. To identify a phenotype of PP5 depleted HDFs, we transfected an siRNA targeting PP5 and performed a proliferation assay using BrdU (Bromodeoxyuridine).

Finally, in order to demonstrate a direct interaction between PP5 and miRNA-663, we cloned a 485bp fragment of the 3'UTR (bearing the three indicated binding sites) into the Luciferase reporter vector psiCheck2 and created a mutated construct for reference.

3 MATERIALS AND METHODS

3.1 Cloning

To monitor the effect of miR-663 on the expression of its assumed target, a 485bp fragment of PP5 mRNA 3'UTR (carrying three possible binding sites) was cloned into a reporter vector: psiCheck™-2 (Promega).

PsiCheck2 encodes genes for two luciferases: modified *Renilla* luciferase (hRluc) and firefly luciferase (FFluc). A multiple cloning site in the 3'UTR of hRluc allows introducing a supposed miRNA-binding sequence to detect a regulation of hRluc expression. FFluc is constitutively active and functions as an intraplasmid reporter for normalization.

Thus, if there is an interaction between the cloned region and a miRNA, the expression of *Renilla* luciferase (being translationally repressed via RNAi) would be diminished as opposed to the signal of firefly luciferase.

3.1.1 Polymerase chain reaction - PCR

3.1.1.1 Amplification of 485bp 3'UTR of human PP5 for cloning

To amplify the genomic insert for psiCheck2 *Thermophilus aquaticus* (*Taq*) DNA polymerase (Biotools Polymerase kit) was used.

The primers for directional cloning of 3'UTR of PP5 (see Appendix) were designed to include restriction sites for the endonucleases *Xho1* and *Not1,* bringing the total size to 503bp for the amplicon. This facilitates ligation with psiCheck2 vector backbone bearing the same restriction sites in its multiple cloning region. Human genomic DNA served as a PCR template, nuclease free water (NFW) as a no template control.

Biotools PCR Kit	**Per reaction**
Template (gDNA)	1 µl
Biotools Polymerase	0.125 µl
Biotools Buffer (2x)	2.5 µl
dNTPs (10mM)	0.5 µl; [0.2mM]
Cloning_PPP5C_fwd/rev	0.5/0.5 µl; [0.2 ng/µl]
$MgCl_2$ (50mM)	1 µl; [2mM]
Nuclease Free Water	18.875 µl
	25 µl

Biotools Temp. profile:	**T [°C]**	**t**
	94	5 min
35 cycles	94	30 s
	60	30 s
	72	30 s
	72	5 min
	4	pause

Table 1: Volumes of reagents and conditions used per PCR sample to amplify 3'UTR of PP5 for cloning

3.1.1.2 Establishment of qPCR for human PP5

The primers for quantitative Realtime PCR (qPCR) were designed to bind in two exons flanking a large intronic sequence which cannot be amplified under given PCR parameters and result in a short product (177bp) for mRNA. They were tested using the Biotools PCR kit under above mentioned conditions (see **Table 1**) with cDNA and gDNA for a template.

3.1.2 Agarose gel electrophoresis

To survey the outcome of PCR or to purify DNA from enzymes, the samples were mixed with DNA Loading Dye (6x) and run on 1% agarose gels (TAE buffer, stained with 1:20 000 Ethidium Bromide) in TAE buffer applying a voltage of 90 V.

3.1.3 DNA purification

After gel electrophoresis the bands were visualized using UV light and fragments of correct size were cut out from the gel with a scalpel. Following the instruction for Wizard® SV Gel and PCR Clean-Up System (Promega) the piece of gel was dissolved and the DNA was eluded in nuclease free water. DNA was kept at 4°C for a short period of time or at -20°C for long term storage.

3.1.4 Quantitation of DNA/RNA

The concentration of DNA respectively RNA was determined by applying 2 µl of sample to a Peqlab Nanodrop – a spectrophotometer which quantifies the amount of nucleic acids based on absorbance at 260 nm and 280 nm.

3.1.5 DNA restriction

To ligate the 3'UTR of PP5 into psiCheck2, vector and insert were digested with Endonucleases *Xho1* and *Not1* at 37°C overnight. Subsequently the sample DNA was separated on a gel and purified using Wizard® SV Gel and PCR Clean-Up System (as described above).

DNA restriction	Per reaction
PCR product	22 µl
NEB Puffer 3 (10x)	3 µl
BSA (1:10)	3 µl
Xho1 / Not1	1 µl / 1 µl
	30 µl

Table 2 Volumes of reagents used for Co-restriction of the insert

3.1.6 Alkaline Phosphatase treatment

The vector (psiCHECK™-2) was additionally dephosphorylated by Calf Intestine Phosphatase (CIP) treatment for 90min at 37°C to avoid religation. Thereafter CIP was removed by electrophoresis and gel purification.

Alkaline phosphatase	Per reaction
vector psiCheck2 (82,83ng/µl)	52 µl
Buffer 3 – NEB (10x)	6 µl
CIP- NEB	2 µl
	60 µl

Table 3 Volumes of reagents for vector dephosphorylation

3.1.7 DNA Ligation

For the ligation of vector backbone and insert an approximate molar ratio of 1/3 (vector/insert) was utilized and incubated with T4 ligase for one hour at room temperature. A vector sample without added insert served as negative control.

DNA ligation	Per reaction
Insert (8.43 ng/µl)	6 µl
vector psiCheck2 (32.76 ng/µl)	6 µl
T4 Ligase buffer (10x)	2 µl
T4 Ligase (1:10)	1 µl
NFW	5 µl
	20 µl

Table 4 Volumes of reagents used for ligation

3.1.8 Precipitation of the ligation sample

In order to avoid failure of electroporation due to high salt concentrations, the ligation samples were precipitated and washed before:

Precipitation of DNA in 20 µl sample:
Add 10 µl NaAc (3M) pH: 5.2
Add 70 µl Ethanol (96%)
Incubation for 1h at -20°C
Spin at 16.000 g for 10 min at 4°C
Discard supernatant
Add 200 µl Ethanol (70%) to wash the pellet
Spin at 16.000 g for 5 min at 4°C
Discard supernatant
Air dry pellet
Resuspension in 5 µl NFW

Table 5 Protocol for precipitation and purification of DNA

3.1.9 Transformation

After thawing of electro competent *E. coli* DH5α[2] on ice, 40 µl were placed in a cuvette and 2 µl of ligation sample (or 1 µl for positive control = psiCHECK™-2) were added.

The following parameters were used on a BTX Electroporator for transforming DH5α:

Transformation parameters:	
voltage:	2500 V, HV
resistor	200 Ω
capacitor	25 µF
cuvette length	2 mm

Table 6 Electroporation Settings for transformation of DH5α

Immediately after electroporation, 450 µl SOC medium (pre-warmed to 37°C) was added and the samples were incubated for 1h at 37°C. Then the transformed bacteria on were plated on LB agar plates (100 µg/ml Ampicillin) to select for vector uptake and incubated at 37°C overnight.

Transformant colonies were transferred to a master plate on the next day and a PCR screening (using Biotools kit with primers "psiCheck2_sequencing_sense/as") was performed (parameters see **Table 7**). Furthermore, 3ml of liquid LB medium (100 µg/ml Ampicillin) were inoculated for overnight cultures to perform a small scale plasmid preparation (Mini-prep). Vector products were verified by sequencing.

Biotools Temp. profile:	**T [°C]**	**T**
	94	2 min
35 cycles	94	30 s
	60	30 s
	72	1 min
	72	5 min
	4	pause

Table 7 PCR cycles in colony PCR screening

3.1.10 QuikChange Site-directed DNA mutagenesis

Following completion of the reporter vector construct carrying the 3'UTR of PP5, a site directed mutagenesis on the predicted miR-663 interaction sites was performed (by using QuikChange ® Multi Site-Directed Mutagenesis kit, Stratagene). This control was designed to attribute a possible effect on luciferase activity specifically to the interaction of miR-663 with the 3'UTR of PP5.

[2] F-, ϕ80dlacZΔM15, Δ(lacZYA-argF)U169, deoR, recA1, endA1, hsdR17(rk-, mk+), phoA, supE44, λ-, thi-1, gyrA96, relA1

3.1.10.1 Overview

In a first step, the DNA of choice (psiCheck2_3'UTR PP5 vector construct) is denatured and mutagenic primers (carrying mismatches) anneal to the desired sites along the single stranded plasmid.

For a next step, the primers are extended and the resulting nicks between the extension products are ligated using the QuikChange Multi enzyme blend. By this, an imperfect copy of the original plasmid is created, carrying the intended mutations (See **Figure 5**).

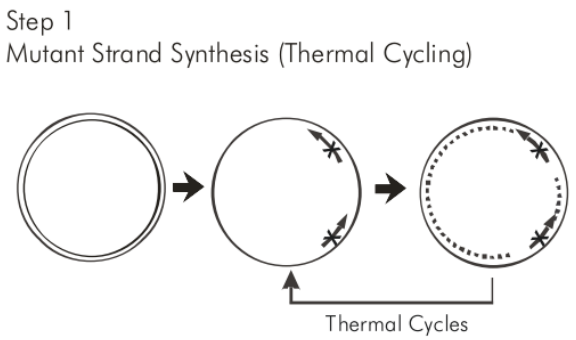

Figure 5: Step 1 of QuikChange Multi Site-directed Mutagenesis, Stratagene Instruction manual #124003a

To degrade the original plasmid, the products are treated with DNA endonuclease *Dpn*I. *Dpn*I is specific for *dam* methylation occurring as a characteristic DNA trait at 5´-**G**m^6**ATC**-3´on DNA originating from *E. coli*. The newly – in vitro - synthesized (mutated) strand does not show this methylation pattern and will consequently not be degraded (see **Figure 6**).

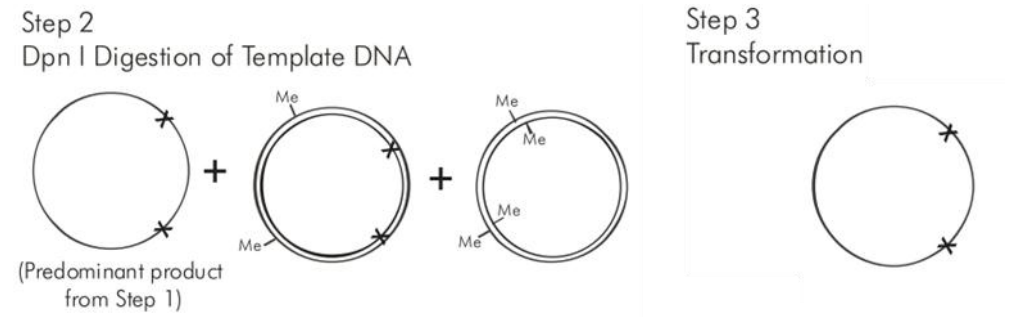

Figure 6 Step 2 and 3 of QuikChange Multi Site-directed Mutagenesis, Stratagene Instruction manual #124003a

In the final step, the mutated single strand plasmid DNA is transformed into XL 10-Gold ultra-competent *E. coli* provided with the kit, where the second strand synthesis and amplification takes place (**Figure 6, Step 3**).

3.1.10.2 Experimental details – mutant strand synthesis

We used three mutagenic primers (see Appendix) to mutate three bases within the seed region (GCG to TAT resulting in a gap for primer binding) of the possible miR-663 binding sites in one step (see **Figure 7**). The kit provides a control set in which the *lacZ* reporter-gene in vector bluescript II SK is disrupted by three stop codons which are repaired with mutagenic primers. Transformation colonies of *E. coli* XL 10 gold, that received the control plasmid with restored *lacZ,* show a blue phenotype on IPTG-X-gal plates and can be used to estimate the success of the mutagenesis reaction.

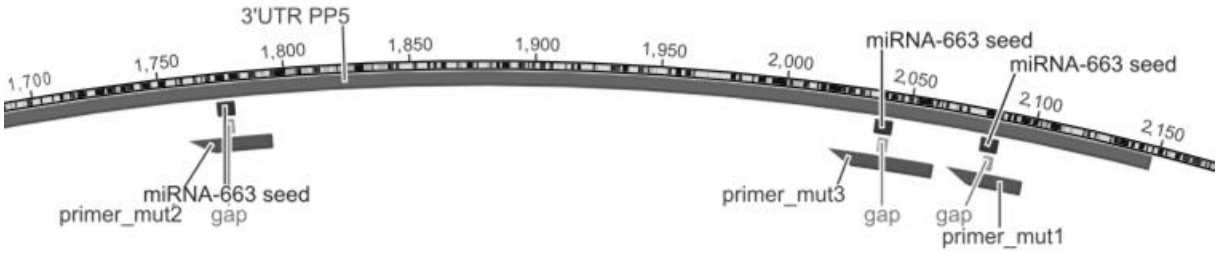

Figure 7 Graphical representation of mir-663 seed regions on 3'UTR of PP5 and their respective mutagenic primer binding sites in the context of the reporter gen construct psiCheck2_3'UTR_PP5

psiCheck2 mutagenesis	Per reaction
10x QuikChange Multi Buffer	2.5 µl
H_2O	14.9 µl
psiCheck2_3'UTR_PP5 (540 ng/µl)	1.85 µl
PPP5C_mut primer 1 (100 ng/µl)	1 µl
PPP5C_mut primer 2 (100 ng/µl)	1 µl
PPP5C_mut primer 3 (100 ng/µl)	1 µl
dNTPs	1 µl
QuikChange Multi enzyme blend	1 µl
Quik Solution (template > 5kb)	0.75 µl
	25 µl

Bluescript II SK (control)	Per reaction
10x QuikChange Multi Buffer	2.5 µl
H_2O	18.5 µl
QuikChange Multi control template (50ng/µl)	1 µl
QuikChange Multi control primer mix (100ng/µl)	1 µl
dNTPs	1 µl
Multi enzyme blend	1 µl
	25 µl

Table 8: Reagents used for mutagenesis of mir-663 binding sites in the 3'UTR of PP5 and respective control

After the reactions were mixed the mutant strand synthesis was carried out using the PCR parameters provided in **Table 9**. For the primer elongation (at 65°C) the QuikChange protocol suggested 2 min per 1kb of plasmid DNA. Although the total size of psiCheck2_3'UTR_PP5 is 6746bp, we decided to only elongate for 10 minutes every cycle.

QuikChange Temp.profile:	T [°C]	T
	95	1 min
30 cycles	95	1 min
	55	1 min
	65	10 min
	4	pause

Table 9 Thermocycling protocol for Mutant strand synthesis

Following the mutant strand synthesis, the original – *dam* methylated – plasmid was degraded by addition of 1µl of *Dpn* I and incubation at 37°C for one hour.

3.1.10.3 Experimental details – Transformation of *E. coli* XL10 Gold

The transformation of *E. coli* XL10 gold was carried out according to the manual (summarized in **Table 10).** Of bacteria transformed with the mutated reporter vector construct (psiCheck2_3'UTR_PP5_mut), 100µl, 10µl and 1µl were used for plating on LB Amp (100 µg/ml) medium. Both for transformation control (puc18) as well as for the mutagenesis control (bluescript II SK_lacZ) 5µl of the bacteria were plated to LB Amp or LB Amp containing X-Gal and IPTG respectively to enable blue-white screening for restored *lacZ* expression in bluescript II SK_lacZ.

We chose 10 colonies of the psiCheck2_3'UTR_PP5_mut transformants (10µl plate) to inoculate 3ml LB medium (100µg/ml Ampicillin) for small scale plasmid preparation and sent the obtained samples for sequencing to verify successful mutagenesis.

QuikChange mutagenesis – Transformation of XL10 gold
Thaw ultracompetent *E. coli* strain XL10 Gold on ice
Per reaction transfer 45 µl of bacteria to prechilled Falcon 2059 polypropylene vials
Add 2 µl of β-mercapto-ethanol
Incubate on ice for 10min
Add 1.5 µl of *Dpn* I digested mutated plasmid (1 µl for puc18 control)
Incubate on ice for 30min
Heat shock bacteria in 42°C water bath for 30 sec
Incubate on ice for 2 min
Add 500 µl NZY-Broth
Incubate at 37°C on mild shaking for 1h
Plate on LB medium + Amp (+ 20 mM IPTG, X-Gal [80 µg/ml] for the mutagenesis control)
Incubate on 37°C overnight

Table 10 Transformation of XL10 gold from QuikChange mutagenesis kit

3.1.11 Plasmid Preparation

For a small scale plasmid preparation (Mini-prep) the Promega Wizard® Plus SV Miniprep DNA Purification System was applied: following alkaline lysis of the bacteria, DNA is obtained by a silica-membrane based column purification. All the steps were carried out in accordance with the manual and DNA was typically eluded in 40 µl of nuclease free water (NFW). To check integrity and directionality of the insert, several plasmid stocks were sent for sequencing. Glycerol stocks of verified clones were kept at -80°C.

In order to obtain endotoxin free plasmids that can be used in cell culture, a larger scale plasmid preparation (Maxi-prep) was performed using Quiagen EndoFree Plasmid Maxi Kit. Therefore a pre-

culture of 3ml liquid LB medium (100 µg/ml Ampicillin) was prepared (8h at 37°C under mild 200 rpm shaking) and then added to 100 ml medium to incubate at 37°C overnight. The next day, Maxi-prep was performed following the kit instructions.

3.2 Cell culture

3.2.1 Culture of HDF5

The human dermal fibroblasts (HDF) that were used for the following experiments originated from one donor ("donor 5") and are adherent cells that grow in a monolayer. We cultured them in Roux-flasks of various dimensions under 37°C, 5% CO_2 (normal culture conditions) in an incubator.

Whenever they reached confluence of about 90%, they were washed twice with sterile PBS and detached by addition of 0.1 % trypsin (in PBS). After a few minutes of incubation at 37°C, 5% CO_2, the cells were taken up in full medium (see Appendix) and split either 1:2 or 1:4 to new flasks.

3.2.2 Determination of cell numbers

After detachment (see above) the cells were suspended in 10ml of full medium. An aliquot of 0.5 ml was blended with 100 µl Trypane-blue to stain dead cells (cells with an intact cell membrane are able to exclude Trypane blue). 20 µl of that mixture were then used to fill a Bürker-Türk counting chamber and cell number was determined under the microscope. The concentration of cells/ml was calculated as follows:

$$concentration\ of\ cells\ per\ ml = \frac{total\ number\ of\ cells\ counted}{number\ of\ large\ squares\ counted} x\ 12\ 000$$

3.2.3 Transfections

3.2.3.1 miRNA transfection using SiPort Neo FX

Delivery of miRNA into HDF5 and HeLa was accomplished by using SiPort Neo FX Reverse Transfection Reagent (Ambion). It is a cationic lipid based transfection reagent, that bases on the principle that RNA/DNA is negatively charged and forms complexes with the positively (cationic) charged lipids that can merge with the cell membrane to deliver the nucleic acids.

SiPort Neo FX is specifically designed for reverse transfection: cells are harvested as described, a suspension with the indicated cell numbers is prepared and cells are added directly onto the lipoplexes. Therefore cells do not need to be seeded the day before.

The transfection reagent and the miRNA for transfection were separately diluted in a serum free basal medium (Optimem, Invitrogen) and incubated for 10 minutes. Following this first incubation, we subdivided the reagent mix and gently added the RNA-mix to promote formation of the transformation complexes. After another 10 minutes, the transfection liposomes were transferred to the bottom of the wells and overlaid with cell suspension. All these steps were carried out at room temperature, subsequently the plates were tilted mildly before incubation under normal culture conditions.

Solutions per well:	6-well plate	12-well plate	24-well plate	96-well plate
SiPort Neo FX	5 µl	3 µl	1 µl	0.5 µl
Optimem	95 µl	47 µl	24 µl	9.5 µl
miRNA (or control) [10µM]	7.5 µl [30 nM]	3 µl [30 nM]	1.5 µl [30 nM]	0.1 µl [10 nM]
Optimem	92.5 µl	47 µl	23.5 µl	9.9 µl
Cells (in medium)	2 x 10^5	0.8-1.2 x 10^5	4 x 10^4	6 x 10^3
Total volume	2.5 ml	1 ml	500 µl	100 µl

Table 11 Volumes and cell numbers used for HDF5 transfection with SiPort Neo FX

For overexpression of miR-663, we transfected the cells with an oligonucleotide mimicking pre-miR-663 and a scrambled miRNA (premiR neg. Ctrl #2) for negative control (Ambion). To estimate the transfection efficiency by FACS (Fluorescence Activated Cell Sorting), a famylated non targeting miRNA (premiR neg. Ctrl #2-FAM) or a cy3-tagged miRNA were used (Ambion).

3.2.3.2 Plasmid transfection using Metafectene Pro

For plasmid based transfection of HDF5 and HeLa cells, Metafectene Pro (Biontex) was used:

The cells were seeded at cell numbers or density as indicated in **Table 12** and incubated overnight under normal conditions. For transfection, Metafectene Pro and DNA were diluted in PBS buffer.

The transfection reagent was prepared as a mastermix, divided into several tubes and the plasmid dilution was added accordingly to them.

After 20 minutes of incubation, the transfection complexes were added to the cells (previously supplied with fresh medium) in drop wise manner. Initially we observed high cell mortality after transfection - uptake of artificial lipids can be toxic to the cells – so we replaced the medium 4h after the transfection as suggested by the manufacturer as an optional step.

Solutions per well:	12-well plate	24-well plate	96-well plate
Metafectene Pro	3 µl	2 µl	0.6 µl
PBS	47 µl	28 µl	19.4 µl
Plasmid DNA	1 µg (* µl)	0.5 µg (*µl)	0.1 µg (*µl)
PBS	50-*µl	30-*µl	20-*µl
Cells (preseeded 24h earlier)	2 x 10^5 in 1 ml	1:1,5 – 1:3 split	1:1,5 – 1:3 split
Total volume	1 ml	500 µl	100 µl

Table 12 Volumes and cell numbers used for HDF5 transfection with Metafectene Pro

3.2.3.3 Plasmid transfection using Lipofectamine 2000

As an alternative to Metafectene Pro, we used Lipofectamine 2000 (Invitrogen) to deliver psiCheck2 vector DNA to HDF5.

In accordance with the manufacturer protocol, we diluted the transfection reagent as well as the DNA in Optimem and incubated for 5min at room temperature. After mixing the two dilutions they were kept at room temperature for 20min. Finally the formed lipoplexes were transferred onto the cells seeded the day before and were distributed equally by gentle tilting of the plate. Four hours afterwards, the transfection medium was replaced by normal growth medium.

Solutions per well:	12-well plate	96-well plate
Lipofectamine 2000	4 µl	0.5 µl
Optimem	96 µl	24.5 µl
Plasmid DNA* various concentrations	1.6 µg*	200 ng*
Optimem	100-*µl	25-*µl
Cells (in medium)	1:1,5 seeded	1:1,5 seeded
Total volume	1 ml	100 µl

Table 13 Volumes and cell numbers used for HDF5 transfection with Lipofecatime 2000

3.2.3.4 Co-transfection with HiPerFect

Quiagen HiPerFect transfection reagent was used in order to transfect HDF5 with plasmid DNA and miRNA in one step.

For this purpose DNA and RNA solutions in HBS buffer (150mM NaCl, 20mM Hepes, pH: 7,4) were prepared. The Transfection reagent was diluted in HBS buffer and set aside at room temperature for

5min. After mixing and incubation for 10 minutes, the HDF5 medium was exchanged and the formed Lipoplexes were added onto the preseeded cells.

Solutions per well:	12-well plate
HiPerFect	6 µl
HBS	44 µl
200ng Plasmid*	* µl
75ng miRNA [10mM]	0.6 µl
HBS	49.4-*µl
Cells (preseeded 24h earlier)	1.2 x 10^5
Total volume	1 ml

Table 14 Volumes and cell numbers used for HDF5 transfection with HiPerFect

3.2.3.5 siRNA transfection with DharmaFECT® Duo

To deliver siRNA, in order to target PP5 mRNA via RNAi, we applied DharmaFECT ® Duo Transfection Reagent by Thermo Scientific. Following the manufacturer instructions, we seeded the cells the day before and exchanged their medium before addition of the lipoplexes.

For the transfection, we separately diluted DharmaFECT reagent and siRNAs in Optimem and left the solutions to incubate for 5min at room temperature. In succession the RNA dilution was added to the transfection lipids and mixed by gently pipetting up and down. After the 20min the lipoplexes had formed and were added to the cells.

Solutions per well:	12-well plate
DharmaFECT Duo	2 µl
Optimem	98 µl
siRNA [20mM]	1.25 µl [25 nM]
Optimem	98.75 µl
Cells (preseeded 24h earlier)	1 x 10^5
Total volume	1 ml

Table 15 Volumes and cell numbers used for HDF5 transfection with DharmaFECT duo

3.2.4 Harvesting cells

To observe influence of the siRNA or miRNA-transfection on the cells, they were harvested 24 to 72 hours afterwards by washing and trypsinization as described und 3.2.1. After detachment, the cells were suspended in full medium, spun down by centrifugation at 170g for five minutes and taken up in PBS to be further prepared for RNA and protein isolation, Lumimetry or FACS.

3.3 Analytical methods

3.3.1 Analysis of RNA

3.3.1.1 RNA Isolation

For RNA isolation the cells were harvested as described (3.2.4) and washed with PBS once more to remove debris and residual medium. Depending on the size of the cell pellet, we added 0.5 to 1 ml of TRIzol® reagent and shook the tube to homogenize the content. Finally the samples were frozen at -80°C for storage until RNA isolation was performed:

Before starting, the whole working area and equipment were carefully cleaned and wiped with RNase Zap ® wipes to prevent RNA degradation by RNases. All work with volatile substances was carried out under a fume hood.

The frozen samples in Trizol reagent were thawed on ice and RNA was extracted according to the protocol (as summarized in **Table 16)**.

Protocol for total RNA isolation using Trizol reagent
Add 200 µl of Chloroform per ml Trizol reagent 15 s vigorously shaking on a vortex Incubate for 5 min at room temperature Spin at 12.000 g for 15 min at 4°C
Transfer clear aqueous phase to an RNase free tube Add 1 µl of Glyco Blue™ Add 500 µl of Isopropanol per ml of Trizol reagent to precipitate the RNA Incubate for 10 min at room temperature Spin at 12.000g for 10 min at 4°C
Remove supernatant Add 1ml of Ethanol (70%) to wash pellet Spin at 7500 g for 5 min at 4°C Thoroughly remove supernatant Air dry RNA pellet Resuspend in 30 µl NFW Heat to 55°C for 2 min to regenerate RNA Leave to cool on ice Store on -80°C

Table 16 RNA isolation with Trizol

3.3.1.2 cDNA synthesis of total RNA

In order to detect and quantify RNA via qPCR it has to be reverse transcribed to complementary DNA (cDNA) first. By the use of an RNA dependent DNA polymerase (Reverse Transcriptase) and short primers of a random sequence (random hexamers), a transcription (not amplification!) of the cellular total RNA content to cDNA was performed. For cDNA synthesis, we used the DyNAmo™ cDNA

Synthesis Kit by Finnzymes to transcribe 200ng of total RNA (see **Table 17** for parameters). Subsequently 30µl of nuclease free water (NFW) were added to dilute the resulting cDNA.

DyNAmo cDNA Kit	Per reaction
Template (RNA) in NFW	200 ng in 7 µl
Reverse Transcriptase	2 µl
DyNAmo Buffer (2x)	10 µl
Random hexamer primer	1 µl
	20 µl

DyNAmo Temp. profile	T [°C]	t
	25	10 min
	37	30 min
	85	5 min
	4	5 min

Table 17 Reagents and Thermocycler program for cDNA synthesis

3.3.1.3 cDNA synthesis of miRNAs

To transcribe the small microRNAs in a representative manner, the NCode™ miRNA First-Strand cDNA Synthesis and qRT-PCR Kit (Invitrogen) was applied.

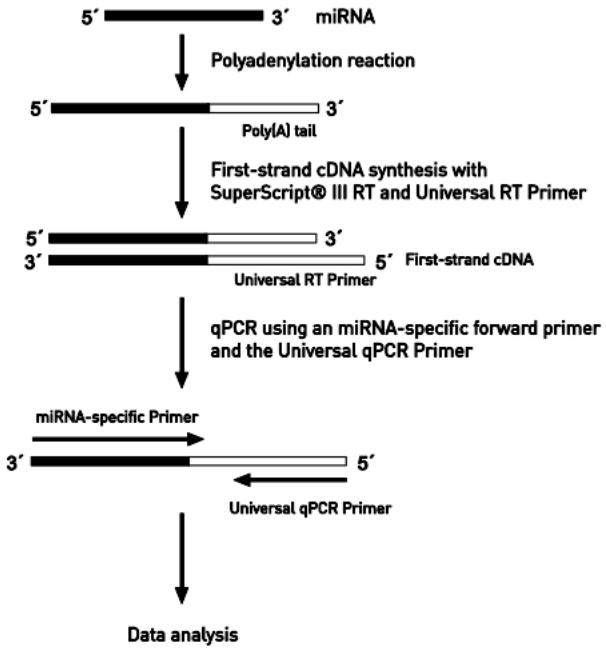

In an initial step, a Polyadenyl-tail is added to all the (mi)RNAs (see **Figure 8**).

This Poly(A) is then bound by RT primer (oligo T), that consequently are elongated by the Reverse Transcriptase (SuperScript™ III RT) and lead to the synthesis of the first-strand cDNA for any miRNAs in the sample.

Specificity for a particular miRNA and its detection is realized in the qPCR: one primer is chosen to bind the miRNA of choice, whereas the second is universal for the Poly(A) sequence added previously.

Figure 8: Work flow of NCode Kit to amplify miRNAs (MAN0000563, Invitrogen)

3.3.2 qPCR

Quantitative (qPCR) or real time PCR is a variant of PCR in which every amplification of DNA is detected due to a fluorescence signal, which allows quantitation of the product. For our experiments we utilized the SensiMix™ SYBR & Fluorescein Kit (Bioline) which uses SYBR Green as a DNA binding stain. This dye has a high affinity to double stranded DNA and only emits fluorescence signal if it is bound. After each cycle of PCR, fluorescence is measured and the cycle number needed for the signal to surpass a certain threshold is determined (Ct values).

qPCR temperature profile and reagent formula are summarized in **Table 18,** primer sequences can be bound in the Appendix. For quality control of qPCR products, the peak profiles in the melting curve were considered.

SensiMix Real Time PCR	Per reaction
Primer (sense/antisense) 10 pmol/µl	0.25 /0.25 µl
SensiMix Real Time buffer	5 µl
cDNA template	1 µl
NFW	3.5 µl
	10 µl

SensiMix Real Time PCR	T [°C]	t
	95	10 min
55 cycles	95	15 s
	60	30 s
	72	15 s
Melting curve	65-99	

Table 18: Reagent mix and temperature profile for pPCR using SensiMix Real-Time PCR Kit (Peqlab)

3.3.2.1 qPCR data analysis

We used an Rcorbett research RG-6000 Light Cycler and quantified the relative expression of target RNA by normalization to a housekeeping RNA (GAPDH mRNA or S5 rRNA respectively for miRNA quantification).

We subtracted the Ct value of the gene of interest from the Ct of the housekeeping gene in the same sample, to normalize for RNA quality and quantity (ΔCt). For comparison we then subtracted the ΔCt value of the chosen control (ΔCt_C) from the ΔCt of the sample of interest (ΔCt_I) to obtain a referenced value ($\Delta\Delta$Ct), which we used to express a fold change taking the logarithmical relation of Ct into account:

$$(1)\ \Delta\Delta Ct = \Delta Ct_I - \Delta Ct_C \qquad fold\ change = 2^{-\Delta\Delta Ct}$$

For error analysis the standard error of the mean (SEM_C, SEM_I respectively) of sample quadruplets (n=4) was determined by division of sample standard deviation (s) by the square root of sample number (n) and calculated according to propagation of uncorrelated errors:

$$(2)\ SEM = \frac{s}{\sqrt{n}} \qquad E_{I-C} = \sqrt{\left({SEM_I}^2 + {SEM_C}^2\right)}$$

3.3.3 Western blotting

For isolation of the protein from harvested cells, two washing steps with PBS were performed and they were pelleted in a 1,5ml reaction tube at 500g for 10min. Subsequently, 50 µl of Nuclear Extraction Buffer (NEB) were added to lyze the cells. By forcing the lysate twice through a QIAshredder column (Quiagen) by centrifugation at 16.000g for two minutes, interfering aggregates

of nucleic acids were broken and the protein extract was collected in Sarstedt tubes and stored at -20°C for further processing.

To obtain information on the expression level of specific proteins in the cell, western blotting was performed. As a prerequisite the total protein concentration for the samples was determined by measuring their absorbance at 280nm on the NanoDrop. Equal amounts (30µg) of protein then were prepared for separation by denaturing Polyacrylamide gel electrophoresis (SDS PAGE). Finally the protein bands were transferred to a PVDF membrane by electro blotting and visualized using specific antibodies.

3.3.3.1 SDS PAGE

Polyacrylamide gel electrophoresis (PAGE) is a biochemical method to separate proteins on a gel due to their mobility in an electric field. By the use of SDS and beta-mercapto ethanol as a reducing agent, the mobility is mainly determined by the size of the protein. Sodium dodecyl sulfate is a detergent that denatures and confers a negative charge to the proteins.

PAA gels consist of a stacking gel - with a low degree of cross links (typically 4%) and a lower PH to concentrate the samples - and the adjacent resolving gel, which has a denser mesh of polyacrylamide polymers (typically 10%), which is responsible for separation according to size. Either custom made gels or commercially available pre-cast gels (NuPAGE™, Invitrogen) were used.

3.3.3.2 Preparation of PAA-gels and electrophoresis

Separation gel (10%)	2 gels
Water	7.5 ml
Resolving-gel-buffer (4x)	3.75 ml
Acrylamide/Bisacrylamide (37.5:1)	3.75 ml
SDS (20%)	75 µl
TEMED	20 µl
APS (10%)	100 µl
Total volume	~15.2 ml

Stacking gel (5%)	2 gels
Stacking-gel premix:	4 ml
TEMED	8 µl
APS (10%)	34 µl
Total volume	~4 ml

Table 19 Preparations of a PAA separation/stacking gel

After thorough mixing, the resolving gel (see **Table 19**) was poured between two glass plates separated by spacers to obtain a defined thickness of 1 mm. The freshly cast gel was covered with 200 µl of isopropanol to accomplish a smooth surface. Following polymerization, we removed the isopropanol and prepared the stacking gel (**Table 19**). We then poured it onto the separation gel and placed a comb to create slots for sample loading.

All the protein samples were mixed with 4x SDS Loading Dye and denatured by the addition of β-Mercapto-Ethanol (1:10) and incubation at 95°C for 10 minutes. They were then cooled on ice and loaded on the gel slots alongside a marker (SeeBlue® Plus2 prestained protein standard) for size reference. Electrophoresis was performed on a Hoefer gel-aperture with a voltage of 200V until the loading-dye front had reached the bottom of the gel (about 45-60 minutes).

3.3.3.3 Transfer

After protein separation by electrophoresis, the stacking gel was removed and filter papers as well as the Roti ®PVDF membrane were accurately sized to fit the gel. To prepare the membrane for protein uptake, it was first activated in methanol for 5 min and then soaked in transfer buffer to equilibrate the pH. Filter paper and gel were wetted with transfer buffer to grant uniform current flow for the transfer.

A Bio-RAD Transblot SD semi dry blotter was used to transfer the negatively charged proteins onto the membrane (see **Figure 9**) at constant amperage of 180 mA for 45 minutes.

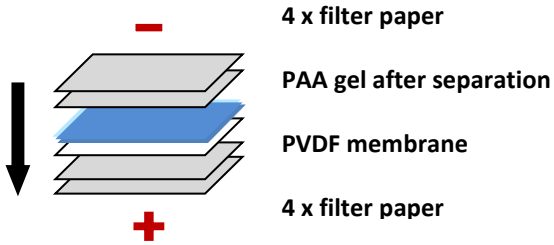

Figure 9: Schematics of the layer arrangement for Western blotting

3.3.3.4 Detection

To visualize the presence of a specific protein a combination of two antibodies is used: the primary antibody, via its antigen binding region, specifically recognizes an epitope on the protein of interest and binds to it. A secondary antibody, designed to target the constant (Fc) region of the primary antibody and conjugated to either an enzyme (e.g. peroxidase), radioactive label or a fluorophore (see **Figure 10**), then recognizes the protein-primary antibody-complex and allows its detection.

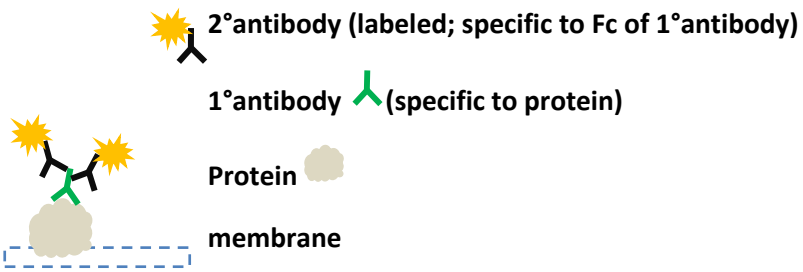

Figure 10 Schematics of an immune detection complex

Prior to incubation with the primary antibody, the membrane was incubated overnight with milk protein (TPBS with 3% milk powder) to reduce unspecific binding of the antibodies to the membrane. After blocking, a dilution of the primary antibody (1:500 mouse anti-PP5/PPt antibody – BD Transduction Laboratories; 1:10 000 rabbit anti-GAPDH antibody, in TPBS 1% milk powder) was administered and incubated for 1,5h at room temperature under a shaker.

Subsequently excess primary antibody was removed by washing three times with TPBS and the secondary antibody (1:5000 anti-mouse peroxidase conjugated antibody; 1:1000 anti-mouse / anti-rabbit Alexa Fluor antibodies in TPBS 1% milk) was added and incubated for 1h. Finally the membrane was washed three times with TPBS.

For visualization of secondary antibodies conjugated to peroxidase (α-mouse-peroxidase antibody) the Pierce ® ECL Western Blotting substrate was prepared according to the instructions, put on the membrane and incubated for 2 minutes in the dark. The luminescence signal, which is created in peroxidase reaction with the substrate, was captured on a Boehringer Lumi-imager F1. To scan for infrared fluorescence for detection of Alexa Fluor secondary antibodies, a Li-Cor Odyssey Imaging System was used.

3.3.4 Flow cytometry

Fluorescence associated cell sorting (FACS) is a biophysical method that uses a laser to detect the properties of particles or cells that flow by in a fluid stream. The scattering pattern, transmission and fluorescence of each cell passing the laser beam are detected and can be used to analyze various parameters.

We used FACS analysis to determine the transfection efficiency (therefore detected fluorescent markers on RNA/DNA) and to assay the entry into S-Phase by BrdU (Bromodeoxyuridine) staining with a labeled antibody. For flow cytometry, the cell suspensions were transferred to round bottom FACS tubes and spun at 170g for 5 minutes. Following the removal of the supernatant, 300µl PBS was used to resuspend the cell pellet.

Exictation was performed using an integrated 488 nm Argon laser. Filters were 530/30nm for FL-1 (FITC, GFP, FAM signal) and 575/26 nm FL-2 (Cy3). Forward scatter and side scatter at 499 nm was used to determine cell integrity. Intact cells were gated and the fluorescence signal was measured in the FL1-H channel to calculate the portion of labeled cells of total living cells.

3.3.5 BrdU (Bromodeoxyuridine) Assay

BrdU is an analogue to the nucleoside thymidine and can be used to monitor the advance in cell cycle of proliferating cells. During replication (S-phase of cell cycle) it is incorporated into newly synthesized DNA and can be detected by specific anti-BrdU antibodies after DNA denaturation.

We measured the fraction of BrdU positive cells by FACS to inquire cell cycle progression of a population. To counterstain dead cells we used Propidium Iodide as an exclusion stain.

Protocol for BrdU-staining of HDF5 for FACS analysis
Incubate cells in tissue culture medium containing 10 µM BrdU for 16 h
Harvest cells by trypsinisation
Spin at 170 g for 10 min ; discard supernatant
Add EtOH 70% (-20°C) dropwise while vortexing to fix cells
Incubate for 30 min at 4°C
Spin at 170g for 10 min ; discard supernatant completely
Add 1ml 2M HCl, 1% Triton (freshly prepared) dropwise while vortexing
Incubate for 30 min at room temperature (for DNA denaturation)
Spin at 170 g for 10 min ; discard supernatant
Resuspend pellet in 1 ml 0,1M NaBorate pH 8.5 (to neutralize pH)
Spin at 170 g for 10 min ; discard supernatant
Resuspend pellet in 150 µl TBS + 3 µl Anti-BrdU antibody
Incubate for 30 min at room temperature
Spin at 170 g for 10 min ; discard supernatant
Wash pellet with 5 ml TBS; spin at 170 g for 10 min ; discard supernatant
Resuspend pellet in 150 µl TBS + 2°AB (anti-mouse FITC 1:100)
Incubate for 30 min at room temperature
Wash pellet with 9 ml TBS; spin at 170 g for 10 min ; discard supernatant
Resuspend pellet in 200 µl PBS, 2.5 µg PI / ml
Transfer to FACS tubes

Table 20 BrdU-staining protocol for flow cytometry

3.4 Luciferase assay

As mentioned above, we carried out a dual Luciferase assay to monitor the effect of miRNA 663 on the expression of a reporter gene (*Renilla* luciferase). Therefore, the 3'UTR of PP5 had been cloned into the psiCheck2 vector downstream of the coding sequence of *Renilla* luciferase. An overview on the experimental setup is given in **Figure 11**.

Renilla luciferase (hRluc) along with the 3'UTR of PP5 ("gene of interest") is transcribed to mRNA. In case a miRNA, due to complementarity of its seed region, binds this composite mRNA, it triggers the intracellular RNAi pathway to degrade the mRNA or impair translation.

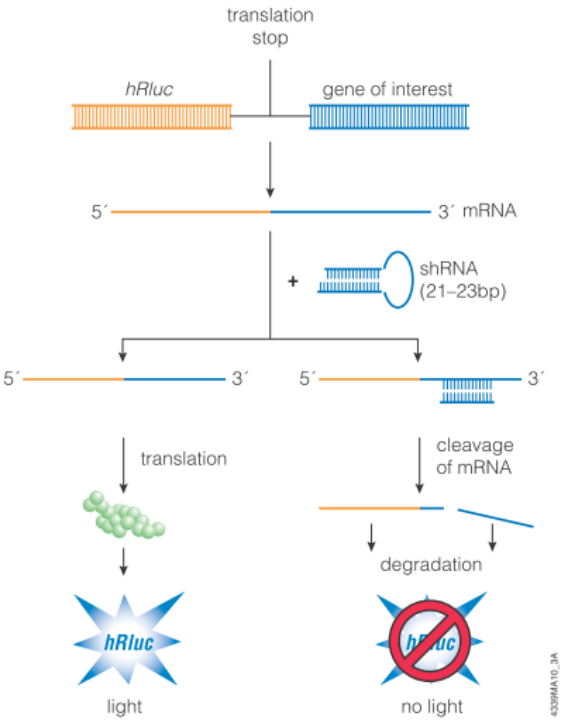

Consequently the hRluc signal decreases depending on the extent of RNAi response which is influenced by interaction potential between miRNA and mRNA.

A second luciferase (firefly luciferase, not shown) is expressed from the same plasmid independently of *Renilla* luciferase and can be used as an internal reference.

Figure 11: Overview on the psiCheck2 luciferase system (Promega TB329,2009)

For the luciferase assay, we harvested the cells as described. The resulting pellet was resuspended in Glo-lysis buffer (room temperature) and lysed for 20-30 minutes. In succession, we transferred the lysate to wells of a black 96-well plate and added the first substrate (Dual-Glo®) just before detection of firefly luciferase signal (on a BioTek-Synergy 2 plate reader).

The subsequent addition of Stop & Glo® substrate stops the firefly luciferase activity and activates *Renilla* luciferase. Finally, the luminescence signal– under influence of the 3'UTR of PP5 – was determined.

3.4.1 Data analysis

Signal intensity of *Renilla* luciferase was first divided by signal of firefly luciferase to normalize for transfection efficiency and intra assay variability. In order to compare between the various reporter constructs, we referenced the ratio (hRluc/FFluc) to the appropriate control by division and calculated a fold change.

For error analysis the standard error of the mean (SEM, see 3.3.2.1, (2)) was calculated and propagated ($E_{I/C}$), M_I and M_C being the mean values for the luciferase signals of the three technical replicates.

$$(3)\quad E_{I/C} = \sqrt{\left(\left(\frac{SEM_I}{M_I}\right)^2 + \left(\frac{SEM_C}{M_C}\right)^2\right)}$$

4 RESULTS

4.1 miRNA-663 and PP5 mRNA in young and senescent HDF5

Preliminary data from a micro array on the miRNA profiles of senescent in comparison to young HDF5 showed an increase in miRNA-663 (Harald Kühnel, unpublished). To confirm this, we performed a Realtime qPCR after cDNA synthesis using the NCode Kit and indeed saw a similar upregulation for miR-663 normalized to 5S rRNA (see **Figure 12**) in senescent cells. To investigate the expression of the presumed target - PP5 - we transcribed total RNA to cDNA using the DyNAmo Kit and found that PP5 mRNA was of 20% lower abundance in senescent cells (see **Figure 13**).

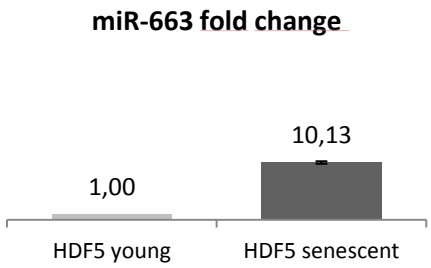

Figure 12 qPCR of NCode transcribed RNA for miR-663 normalized to 5SrRNA in senescent relative to young HDF5.

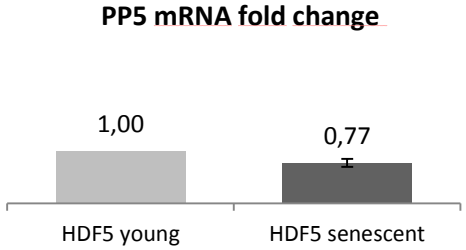

Figure 13 qPCR of DyNAmo transcribed RNA for PP5 normalized to GAPDH in senescent relative to young HDF5.

4.2 Effects of miR-663 overexpression on PP5 protein

Subsequently we determined how overexpression of miRNA-663 affects the protein level of PP5. Therefore we transfected HDF5 with 30nM of miRNA-663 (respectively non targeting miR-Control #2) in 6-well format (2 x 10^5 cells per well) using SiPort NeoFX and harvested the cells 48h post transfection to isolate RNA and protein.

To visualize miRNA delivery upon transfection, we included a cy3-dye labeled non targeting miRNA control (cy3-miR Ctrl), which we detected by fluorescence microscopy (see **Figure 14**).

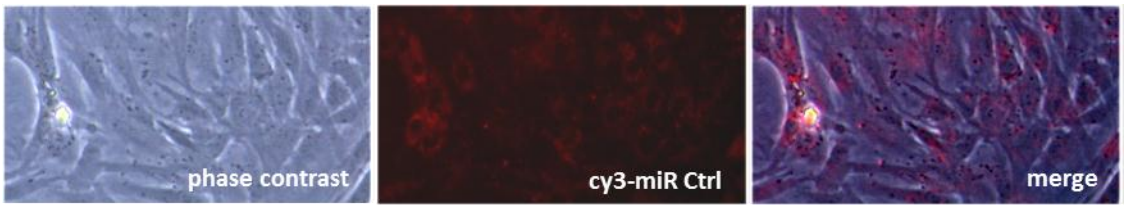

Figure 14: Microscopy images of HDF5 in phase contrast and cy3-miR Ctrl signal (24h after transfection) in the fluorescence channel. The merged image shows cy3-miR Ctrl staining mainly the cytoplasm and not the nuclei.

By qPCR following NCode cDNA synthesis, we were able to demonstrate a more than hundredfold increase in miRNA-663 (**Figure 15**). For detection of protein signal, we used mouse anti-PP5 antibody and rabbit anti-GAPDH antibody as primary antibodies and detected those with anti-mouse/rabbit peroxidase conjugated antibodies.

We used Pierce ® ECL Western Blotting substrate and read out the luminescence signal on a Boehringer Lumi-imager F1. Due to the low signal for the PP5 bands (**Figure 16:** 58kDa, indicated by black arrow), we did not quantify the band intensities.

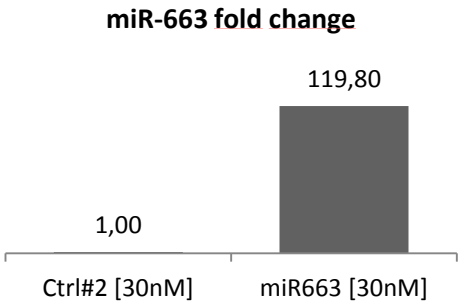

Figure 15 qPCR of NCode transcribed RNA for miR-663 normalized to 5S rRNA in miR-663 (663) and control #2 transfected HDF5, 48h p.T.

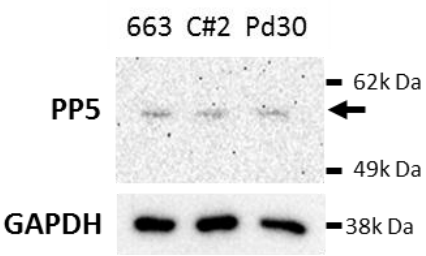

Figure 16 Western Blot for PP5 (indicated by arrow) and GAPDH protein from HDF5 transfected with miR-663 (663), Control #2 (C#2) and cells after 30 doublings (Pd30).

4.3 miRNA-663 overexpression – time course 24h, 48h, 72h

We were interested in how the levels of miRNA-663 change after transfection and addressed this question by qPCR at time points 24h, 48h and 72h post transfection (p.T.) of 30nM miR-663 in a 6-well format (2x10^5 cells per well) using Siport Neo FX.

The abundance of miRNA-663 peaked after 24h and decreased over time (see **Figure 17**), starting from more than 600 fold increase 24h p.T. to about 100 fold, 72h after the transfection. Also PP5 mRNA and protein levels were assessed in this experiment: We were surprised to see a 60% induction of PP5 mRNA 24h p.T. for miRNA-663 transfected as compared to miRNA Control #2 transfected HDF5 (see **Figure 18**). On day 2 and day 3 (**Fig. 18, 48h and 72h**), however, the level of PP5 was only slightly influenced by miR-663 overexpression.

In contrast to PP5 mRNA levels, we observed a decrease in PP5 protein upon transfection of miR-663 on Western blot (**Figure 19**). We quantitated the band intensities (see **Figure 20**) and saw a time dependent decline, starting from a slight reduction 24h p.T. to 20% reduction after 72h.

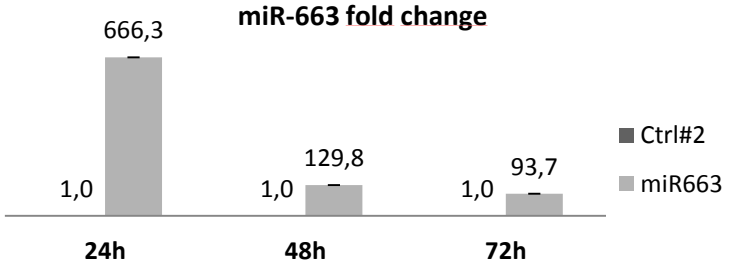

Figure 17 qPCR of NCode transcribed RNA for miR-663 normalized to 5S rRNA in miR-663 and Control #2 transfected HDF5 at time points 24h, 48h and 72h post transfection.

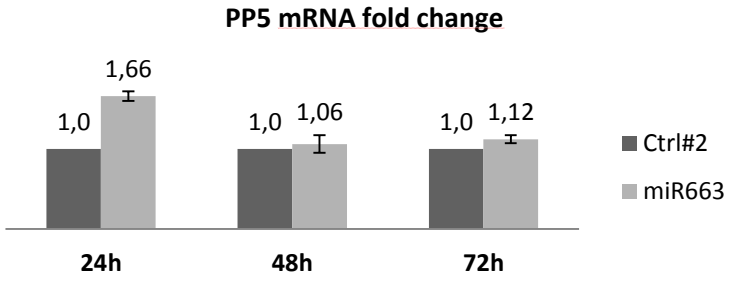

Figure 18 qPCR of DyNAmo transcribed RNA for PP5 normalized to GAPDH in miR-663 and Control #2 transfected HDF5 at time points 24h, 48h and 72h post transfection

.

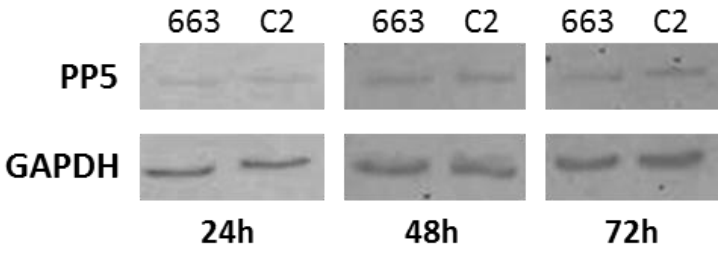

Figure 19 Western blot for protein samples taken 24h, 48h and 72h after transfection of 30nM miR663 (663) and control #2 (C2). Alexa Fluor secondary antibodies were detected by the Li-Cor Odyssey infra-red fluorescence imaging system (700nm for anti-mouse: anti-PP5, 800nm for anti-rabbit anti-GAPDH).

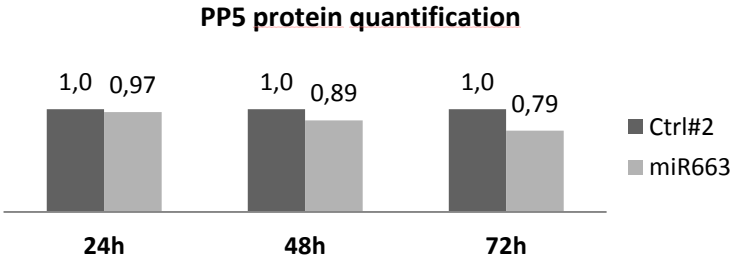

Figure 20 Quantification for Western blot of protein samples taken from HDF5 24h, 48h and 72h after miR-663 transfection (see **Figure 19**).

4.4 miRNA-663 overexpression – [1-30nM]

Surprised by the result of the time course experiment, showing an increase in PP5 mRNA on the more than 600 fold induction of miR-663 **(Figure 17),** we decided to moderate the level of initial concentration.

We transfected HDF5 in 12-well format (8 x 10^4 cells/well) using SiPort Neo FX with 1 nM, 3 nM, 10 nM and 30 nM miR-663 and 30 nM miRNA Control #2. Samples for RNA isolation were harvested 48h post transfection.

In qPCR we saw a clear dose dependent effect for miR-663 transfections (**Figure 21**), although the maximum fold induction was lower than in the 6-well transfected cells from previous experiments. On mRNA level no apparent correlation between molarity and PP5 was detected: while samples transfected with 1 nM and 3 nM of miR-663 both showed about a twentyfold induction in miR-663 levels (**Figure 21)**, the amount of PP5 mRNA appeared reduced to 50% in one, while it was elevated to 200% in the other sample (**Figure 22**). Transfection of miRNA-663 with 10nM or 30nM concentration (corresponding to 70- and 90 fold increase respectively – **Figure 21**) did not influence PP5 mRNA levels much in this setup (**Figure 22**).

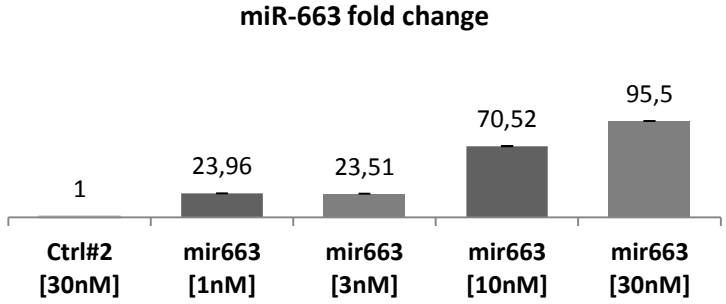

Figure 21 qPCR of NCode transcribed RNA for miR-663 normalized to 5S rRNA in miR-663 and Control #2 transfected HDF5 at concentrations from 1nM – 30nM

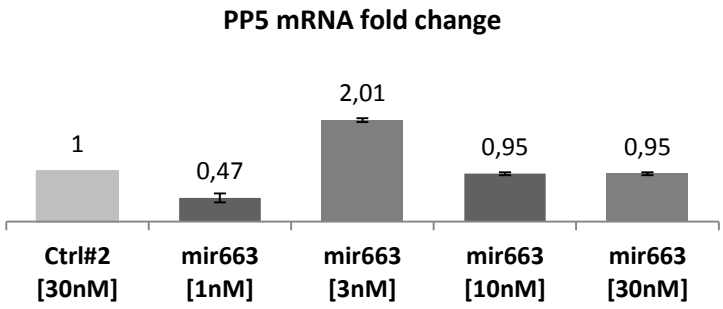

Figure 22 qPCR of DyNAmo transcribed RNA for PP5 normalized to GAPDH in miR-663 and Control #2 transfected HDF5 at concentrations from 1nM – 30nM

4.5 miRNA-663 long term overexpression

Since we were not able to detect any phenotypical changes in cells upon miRNA-663 overexpression in previous experiments, we decided to perform three consecutive transfections of HDF5 with 30nM of miR-663. Knowing that subsequent lipofections put a strain on the cells, we decided to wait for 72h before transfecting the cells anew, using SiPort Neo FX reverse transfection in 12-well format (8x 10^4 cells/well).

On each transfection an aliquot of HDF5 was taken for protein and RNA isolation before the cells were reseeded. Microscopically no change in cell morphology or growth behavior could be observed.

Figure 23 shows the fold changes for miR-663 induction after each transfection: obviously the third transfection (**T3**) was most successful, showing a more than 700 fold increase. After cDNA synthesis we conducted qPCR to determine the levels of PP5 and p21 mRNA, which we also thought could be influenced by prolonged miR663 overexpression.

Again, the results on PP5 mRNA were somehow inconclusive: 72h after the first transfection (**T1**, **Figure 24**), we saw an mRNA reduction of about 1/3rd, hardly any effect after the second transfection (**T2**) and a decrease of about 1/4th for the last transfection (**T3**) as compared to the control miRNA. The mRNA levels of p21 (**Figure 25**) seem to correlate inversely: 72h after the second transfection – in which PP5 mRNA levels in miR-663 transfected cells hardly differ from the control - its expression is reduced to almost 50%. At the lowest value of PP5 (**Fig. 24, T1**) we find p21 mRNA least influenced by miR-663 overexpression (**Fig. 25, T1**).

In contrast, on PP5 protein levels (**Figure 26**) a clear effect of miR-663 overexpression could be detected. Using peroxidase conjugated secondary antibodies, we saw a decrease of 30-40% 72h after each of the miRNA-663 transfections (**Figure 27**). The influence was observed most clearly in the Western blot for the last transfection (**Fig. 26, T3**).

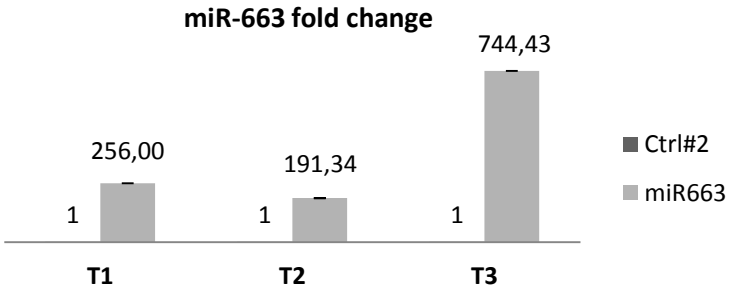

Figure 23 qPCR of NCode transcribed RNA for miR-663 normalized to 5S rRNA in three consecutive transfections (72h interval) of miR-663 and Control #2 (30nM) transfected HDF5.

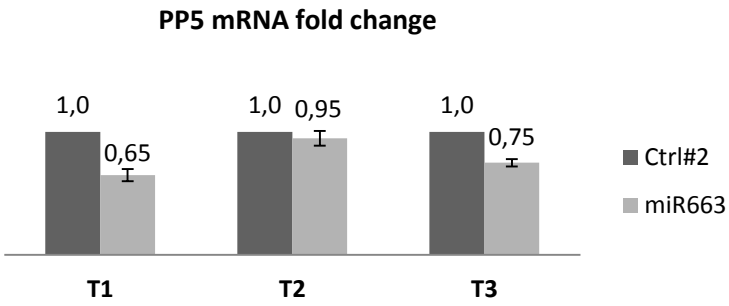

Figure 24 qPCR of DyNAmo transcribed RNA for PP5 normalized to GAPDH in three consecutive transfections (72h interval) of miR-663 and Control #2 (30nM) transfected HDF5.

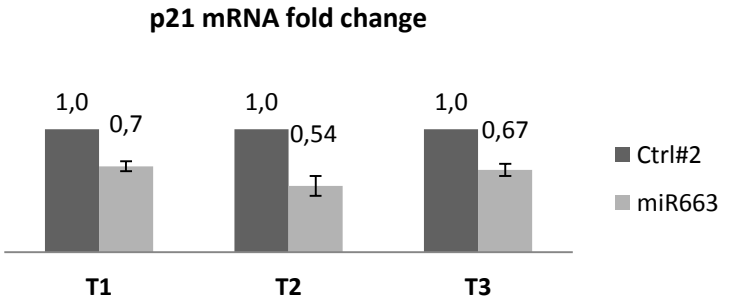

Figure 25 qPCR of DyNAmo transcribed RNA for p21 normalized to GAPDH in three consecutive transfections (72h interval) of miR-663 and Control #2 (30nM) transfected HDF5.

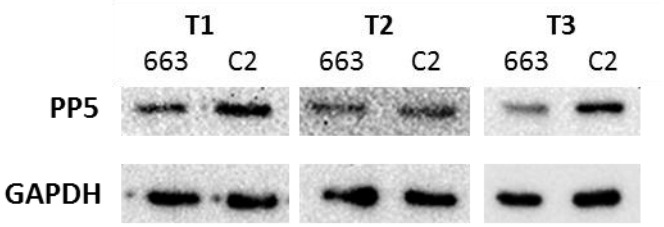

Figure 26 Western blot for protein samples taken 72h after each of three consecutive transfections of 30nM miR663 (663) and control #2 (C2).

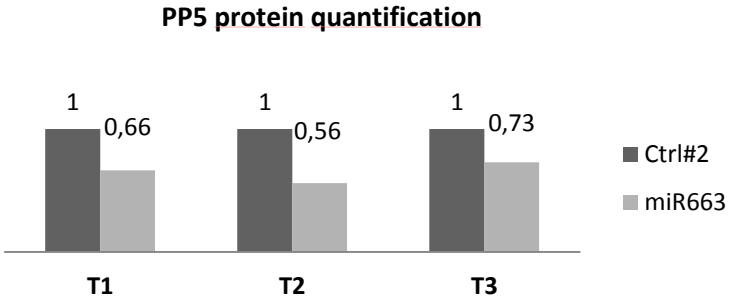

Figure 27 Quantification for Western blot of protein samples from each of three consecutive transfections of 30nM miR663 and Control #2 (see **Figure 21**).

4.6 DNA damage conditions: H_2O_2 treatment

According to our hypothesis the expression of miRNA-663 would aid in establishing a p21 dependent growth stop by preventing the dephosphorylation of $p53^{Ser15}$. Thus, miR-663 induction would be part of a stress response. We aimed to provoke this p53 phosphorylation - as an indication of DNA damage - by treatment with sublethal levels of H_2O_2.

We exposed HDF5 in tissue culture flasks (75cm^2 growth area) to 100µM H_2O_2 for 1h, replaced the treatment medium with full medium and incubated the cells under normal culture conditions. After 4h, 24h and 48h recovery, we took samples of treated and untreated HDF5 for RNA isolation.

As can be seen in **Figure 28**, the fold changes in miR-663 were moderate for the conducted H_2O_2 treatment: after an initial downregulation (4h recovery) to approximately 50%, we saw an increase to a level about 30% higher than for the untreated cells. Within the next 24h, the cellular level of miRNA-663 dropped again to about 40% and we could not observe a restoration to levels of the control within the chosen time frame.

Surprisingly the levels of mRNA for PP5 behaved in a similar manner (see **Figure 29**): Shortly after the treatment, the level of PP5 mRNA dropped to about 80% (4h recovery) and increased to 130% (24h recovery) before going back to 80% (48h recovery).

In qPCR for p21 we observed the largest fold changes upon treatment with 100 µM H_2O_2 (**Figure 30**): Already after 4h of recovery, p21 mRNA was almost fourfold increased, peaking at a more than eightfold level (24h recovery) and declined to about twofold amount on the last time point (48h recovery).

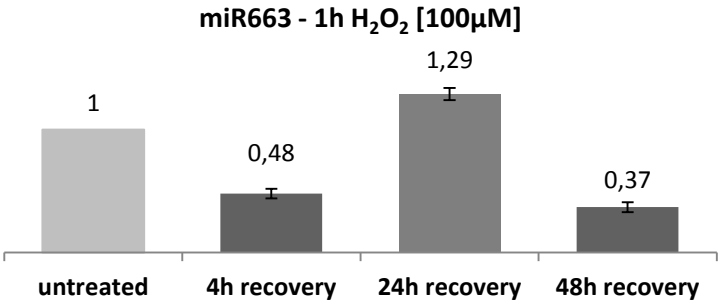

Figure 28 qPCR of NCode transcribed RNA for miR-663 normalized to 5S rRNA in HDF5 after 1h of 100µM H_2O_2 treatment. The fold changes were calculated relative to samples taken from untreated HDF5 at the respective timepoints.

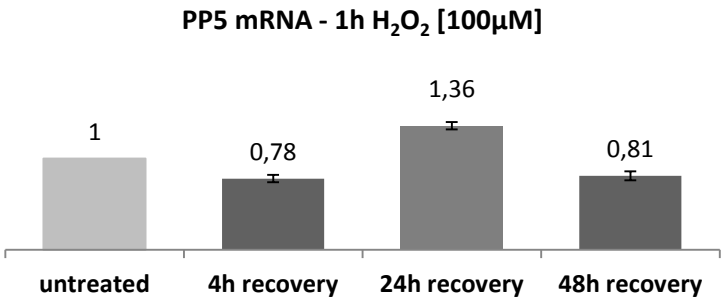

Figure 29 qPCR of DyNAmo transcribed RNA for PP5 mRNA normalized to GAPDH in HDF5 after 1h of 100 µM H_2O_2 treatment. The fold changes were calculated relative to samples taken from untreated HDF5 at the respective timepoints.

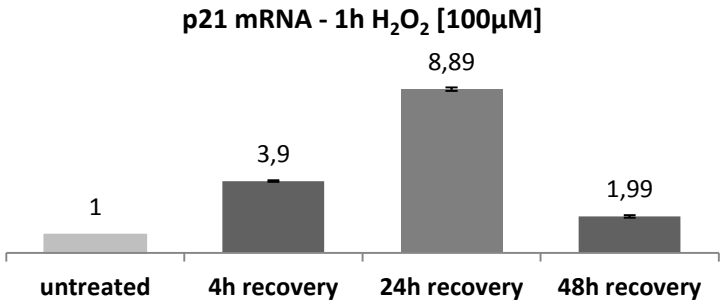

Figure 30 qPCR of DyNAmo transcribed RNA for P21 mRNA normalized to GAPDH in HDF5 after 1h of 100 µM H_2O_2 treatment. The fold changes were calculated relative to samples taken from untreated HDF5 at the respective timepoints

4.7 siRNA targeting PP5

To elucidate a possible phenotype of reduced PP5 levels - which we observed in senescent cells - we applied a siRNA targeting PP5 mRNA to achieve an RNAi mediated knockdown similar to what we thought miRNA-663 would cause.

In 6-well format (2x10^5 cells per well), we transfected HDF5 with 25nM of siRNA-tPP5 and a non-targeting smartpool of siRNA (siR Ctrl#2 sp) using the DharmaFECT reagent. To monitor siRNA delivery we used a famylated siRNA (siGLO green, Dharmacon) and visualized it using a FITC filter on fluorescence microscopy (see **Figure 31**). 24h after transfection we took samples for RNA isolation and transcribed total RNA to cDNA using the DyNAmo Kit.

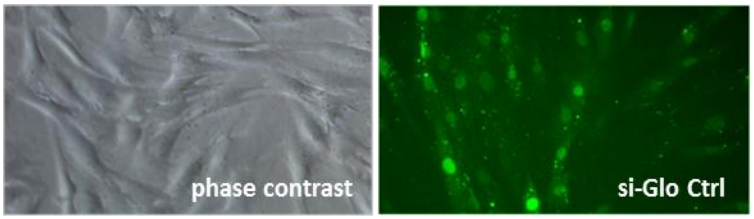

Figure 31 Microscopy image of HDF5 in phase contrast and FITC filter to detect fluorescence si-Glo Ctrl.

Figure 32 shows that the transfection of 25nM siRNA-tPP5 resulted in an efficient knock down of PP5 mRNA (more than 80%) as determined by qPCR. Interestingly, 24h after transfection of siRNA targeting PP5, also the mRNA for p21 was downregulated (**Figure 33)**.

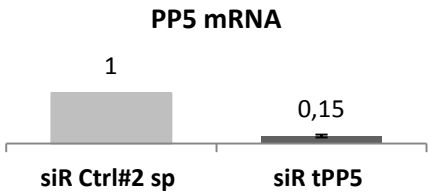

Figure 32 qPCR of DyNAmo transcribed RNA for PP5 in HDF5 after transfection of 25nM siRNA targeting PP5mRNA normalized to GAPDH, relative to siR Ctrl#2 smartpool.

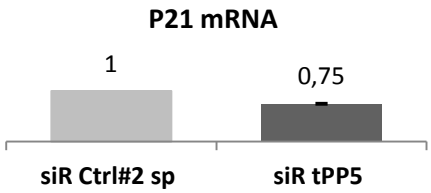

Figure 33 qPCR of DyNAmo transcribed RNA for P21 mRNA normalized to GAPDH in HDF5 after transfection of 25nM siRNA targeting PP5, relative to siR Ctrl#2 smartpool.

4.8 BrdU assay

Since we could not observe any influence of miRNA-663 overexpression on HDF5 growth microscopically, we decided to perform a proliferation assay using BrdU incorporation.

To further elucidate if any effect on cell cycle progression is actually caused by the reduced level of PP5 and not due to other targets of miR-663, we included the siRNA targeting PP5 (siR-tPP5).

We compared the effect of two transfections of HDF5 in 6-well format (2 x 10^5 cells per well): for the first, we introduced 25 nM siRNA-tPP5 and control (siRNA Ctrl#2) using DharmaFECT, in the second one we transfected 30 nM miR-663 (and respective control) with SiPort Neo FX.

24h after the transfections, we harvested the cells and reseeded them (1 x 10^5 per 6-well) with medium containing 10µM BrdU and assessed their entry into S-phase 16h afterwards, by antibody staining of BrdU and FACS detection thereof (assay described under 3.3.5).

Figures 30-34 show the results of flow cytometry in which we determined the fraction of cells that had recently synthesized new DNA (positive for BrdU “in M1”) and were actively proliferating compared to the untransfected control population of cells.

For the transfection of miRNA-663 we observed 76% cells positive for BrdU (**Figure 31**) which hardly differs from the non-targeting control (75%, miR Ctrl#2, **Figure 30**), indicating that there was no effect of miR-663 on S-phase entry in these cells.

In cells transfected with siRNA targeting PP5, the fraction that had already replicated their DNA, accounted for about 69% (**Figure 32**). Unfortunately the siRNA (Ctrl#2), erroneously applied as a control in this experiment (see **Figure 34**), caused a strong proliferative phenotype (48% BrdU positive) due to reported off-target effects. However, of HDF5 that were treated only with the transfection reagent DharmaFECT, also a fraction of 70% were BrdU positive (**Figure 33**) - very similar to siRNA-tPP5 transfected cells.

Summarized, the FACS data indicates, that the delay in cell cycle progression we saw on transfecting miRNA-663 (**Figure 31**, 75%) and siRNA-tPP5 (**Figure 32**, 70%) was most likely caused by the stress of lipofection.

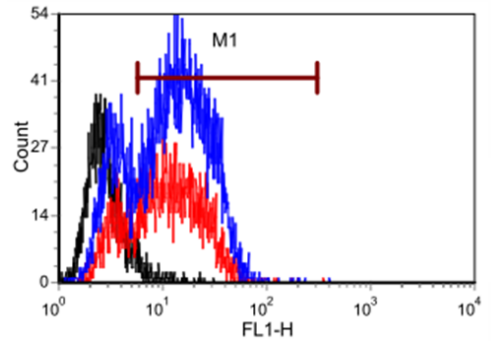

miR Ctrl#2 1	75,8% in M1
miR Ctrl#2 2	74,5% in M1
untransfected	5,4% in M1

Figure 34 FACS histogram of BrdU assay (16h treatment) in HDF5 transfected with 30 nM miRNA Ctrl2.

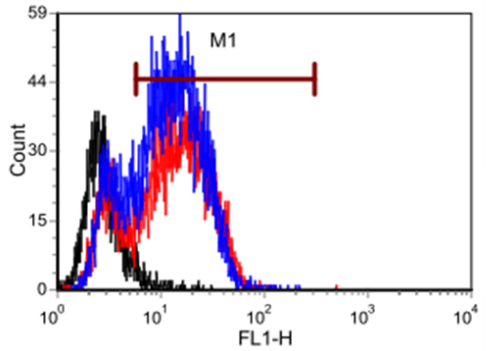

miR-663 1	76,38% in M1
miR-663 2	76,07% in M1
untransfected	5,4% in M1

Figure 35 FACS histogram of BrdU assay (16h treatment) in HDF5 48h after transfection with 30 nM miRNA-663.

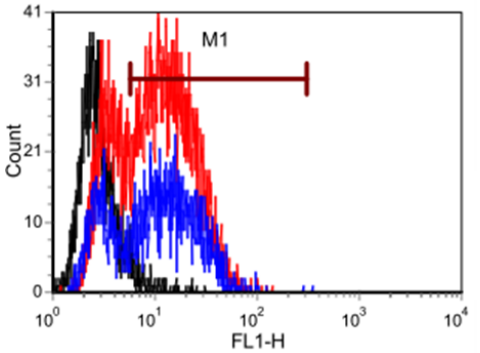

siR-tPP5 1	69,89% in M1
siR-tPP5 2	68,37% in M1
untransfected	5,4% in M1

Figure 36 FACS histogram of BrdU assay (16h treatment) in HDF5 transfected with 25 nM siRNA targeting PP5 (siR-tPP5).

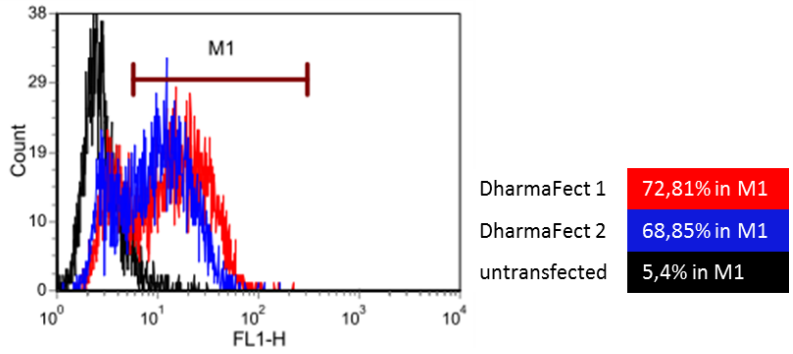

Figure 37 FACS histogram of BrdU assay (16h treatment) in HDF5 treated only with the transfection reagent DharmaFect.

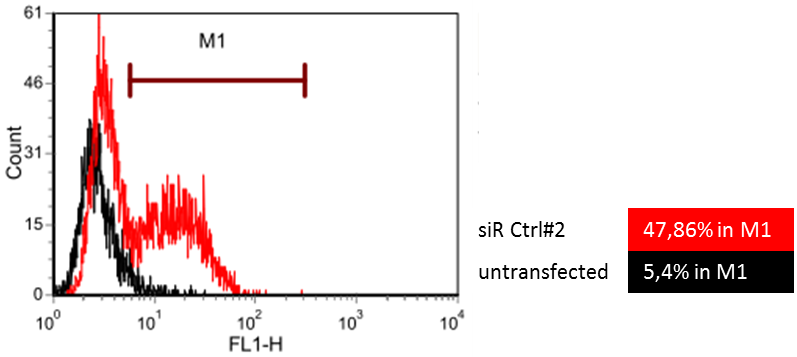

Figure 38 FACS histogram of BrdU assay (16h treatment) in HDF5 transfected with 25 nM siRNA Control #2. The strong proliferation phenotype disqualifies this siRNA as a control!

4.9 Cloning of psiCheck2 reporter gene constructs

4.9.1 psiCheck2_3'UTR_PP5

To assay the interaction between miRNA-663 and the potential target sequences in the 3'UTR of PP5, we first amplified the region of interest (485bp) from genomic DNA extended with a total of 18 base pairs to incorporate restriction sites (5' *Xho1* and 3' *Not1*) for cloning to psiCheck2.

Figure 39 shows the PCR products for primers cloning_PP5_fwd and cloning_PP5_rev on human gDNA and cDNA: a product band at about 500bp corresponded to the expected 503bp fragment and was excised from the gel. After DNA purification from gel (see materials and methods), both vector (psiCheck2) and insert were digested with endonucleases *Xho1* and *Not1* and the vector was treated with alkaline phosphatase (CIP) to prevent religation.

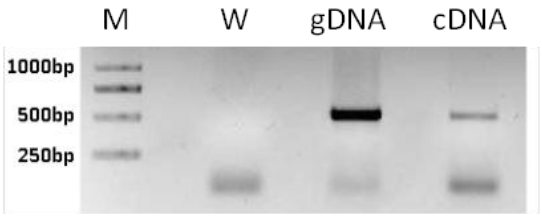

Figure 39 1% agarose gel image of PCR to amplify a 485bp fragment of PP5 3'UTR for cloning. 25 µl Biotools PCR with cloning primers resulted in a strong band for genomic DNA template (gDNA: 1 µl) and a weaker band for cDNA of the expected size (485bp + 18bp extension for restriction sites). For non-template control 1µl of water (W) was used.

After ligation of vector and insert (3.1.7), we precipitated and purified the ligation products and transformed electrocompetent *E. coli* DH5α by electroporation (3.1.9). After plating on agar plates containing 100 µg/ml ampicillin and incubation overnight, we observed 17 colonies for the ligation products and countless numbers (>>1000) for the transformation of 5 ng vector stock.

In **Figure 40**, the outcome of a PCR screening (using primers psiCheck2_sequencing_sense/as) for 6 of these colonies is depicted: positive clones (#1-3 and #5) show a distinct band of approximately 1kb size, corresponding to the 1009 bp amplicon after correct insertion. The PCR product for the empty vector is considerably smaller (506 bp), as can be seen in the lane for untreated Vector (Vu).

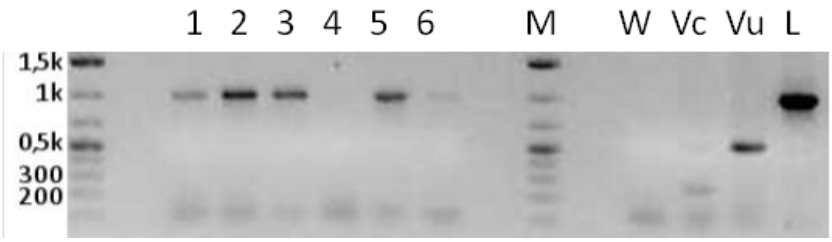

Figure 40 1% agarose gel image of colony screening PCR after transformation of DH5α. Transformation colonies #1, 2 ,3 and 5 show a product of 1kb, from the empty vector (Vu) a 500 bp fragment was amplified. For control, the CIP treated vector (Vc) and an aliquot (1 µl) of the ligation reaction (L) were used. A water sample (W) served as a non-template control.

For the samples that showed strong PCR product bands in the colony screening (Figure 9, #1-3 and #5) we verified the accurate integration by sequencing 15µl of plasmid dilution (150 ng/µl, 2 pmol/µl primer: psiCheck2_sequencing_sense/as) after a small scale plasmid preparation.

4.9.2 psiCheck2_3'UTR_PP5_mut

In order to determine whether any regulation of hRluc expression is a specific consequence of miRNA-663 binding to the 3'UTR of PP5, we decided to mutate the potential binding sites. To accomplish the mutation of bases CGC - complementary to miR-663 seed region - to TAT, we employed the QuikChange Site-directed DNA Mutagenesis Kit (Invitrogen) as described under 3.1.10.

The transfection of XL10 ultra-competent *E. coli* (included in the kit) was characterized by a high transformation efficiency of 1.35 x 10^9 colony forming units (cfu) per µg of plasmid DNA. In vector bluescript II SK, which served as control for primer mediated introduction of mutations, we saw 69% mutagenesis efficiency (see **Table 21**). This meant that for the optimized mutagenesis reaction more than 2/3 of the transformants successfully carried all three mutations. Based on this efficiency, we chose 8 colonies for Mini-prep and sent four of them for sequencing. One of the four samples carried all three desired mutations and the corresponding clone was used for large scale plasmid preparation.

Transformation of XL10 ultra competent cells	cfu (mean)	Transformation efficiency:
puc18 (9x10^-5 ng): 5µl bacteria solution per plate	122	1.35 x 10^9 cfu/µg DNA
bluescript II SK: 10µl bacteria per plate	160 (blue) / 71 (white)	69% mutagenesis efficiency
psiCheck2_3'UTR_PP5_mut: 100µl	>1000	
psiCheck2_3'UTR_PP5_mut: 10µl	152	
psiCheck2_3'UTR_PP5_mut: 1µl	32	

Table 21: Transformation of XL10 ultra-competent *E. coli* after psiCheck2_3'UTR_PP5 vector mutagenesis. For 1 µg of DNA of transformation Control puc18, 1.35 x 10^9 colony forming units (cfu) were calculated. The mutagenesis control bluescript II SK resulted in 160 blue of a total of 231 colonies, showing that 69% of the transformants carried all three mutations.

4.10 Luciferase assay

4.10.1 First application of all vector constructs

For the first implementation of the reporter vector constructs, we reversely transfected 30nM miRNA-663 in a 12-well format (1,2 x 10^5 cells/well) using Siport Neo FX transfection agent. On the following day, we introduced 1 µg of plasmid DNA using Metafectene Pro. After 24h we harvested the cells and conducted the Dual luciferase assay as described under 3.4.

In order to microscopically visualize of miRNA and vector transfection we included a cy3-labelled miRNA control (cy3-miR Ctrl, Dharmacon) and a vector expressing GFP (pmaxGFP by Lonza, see **Figure 41**). While the miRNA delivery seemed to have worked well, we observed a low GFP signal indicating low transfection efficiency for the vector.

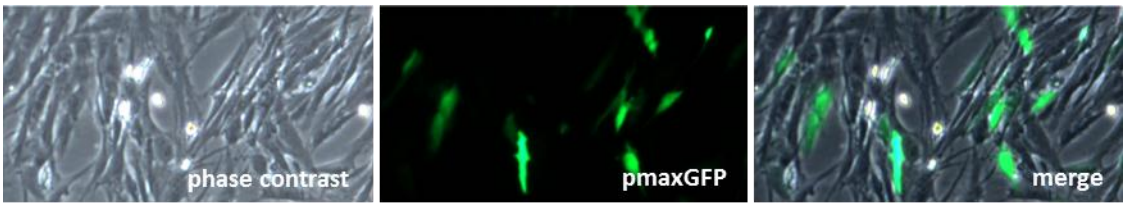

Figure 41: Microscope image of phase contrast and fluorescence FITC channel for the same area of HDF5 transfected with vector pmaxGFP. The merge implies that the transfection efficiency of was rather low.

The result for the Luciferase assay is depicted in **Figure 42**: in the original vector psiCheck2 (psiC2) we saw that the signal for miR-663 transfection was 20% lower than for the non-targeting miRNA control (Ctrl#2). This was a somewhat surprising observation, given that there are no elements on the vector that could be influenced by miRNA-663 itself.

The signal ratio between *Renilla* luciferase expression (Rluc) and vector internal control firefly luciferase (FFluc) was indeed decreased to 85% by miRNA-663 transfection in the reporter vector with predicted binding sites.

However, the mutant 3'UTR did not show the expected rescue of effect but even a slightly stronger decrease of Rluc by miR-663 transfection. Sample intensity values ranged from 1200 to 1900 for FFluc and 400 to 1100 for Rluc.

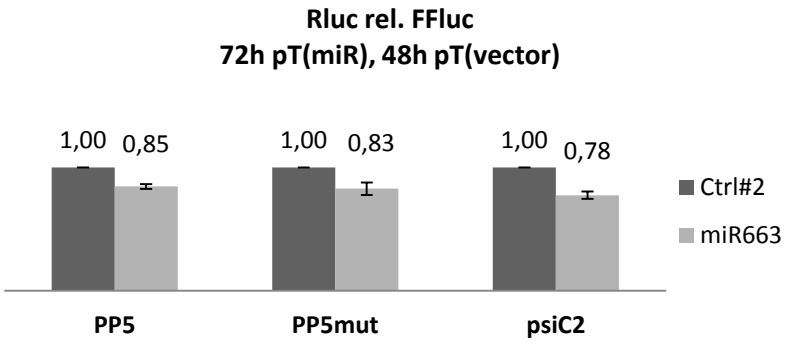

Figure 42 Calculated ratios of *Renilla* and Firefly luciferase signals for reporter vector construct after transfection of 30nM miR-663 relative to miR Ctrl#2. Luciferase was assayed 72h after transfection of miRNA and 48h after vector transfection.

To establish a reliable reporter gen assay, we took several approaches to vary the assay parameters as described below:

4.10.2 Effect of endogenous miRNAs on reporter constructs

We were interested to what extent the *Renilla* luciferase signal (subdued to the 3'UTR of PP5) might be affected by the miRNA levels constitutively present in HDF5.

Therefore we transfected HDF5 in 12-well format (2 x 10^5 cells) with the three reporter vector constructs (psiC2, psiC2_3'UTR_PP5 and psiC2_3'UTR_PP5mut) using Metafectene Pro and monitored luciferase expression 24h thereafter.

Figure 43 summarizes the obtained luciferase ratios: in the original vector (psiCheck2) the *Renilla* luciferase was more than 40% higher expressed than Firefly luciferase, whereas the reporter construct, bearing the 3'UTR of PP5, showed an almost 1:1 ratio in the two luciferase signals.

Mutation of the binding sites for miRNA-663 (**Figure 43,** PP5mut) resulted in an even stronger decrease in *Renilla* luciferase, which could be an indication for RNAi not mediated by miR-663.

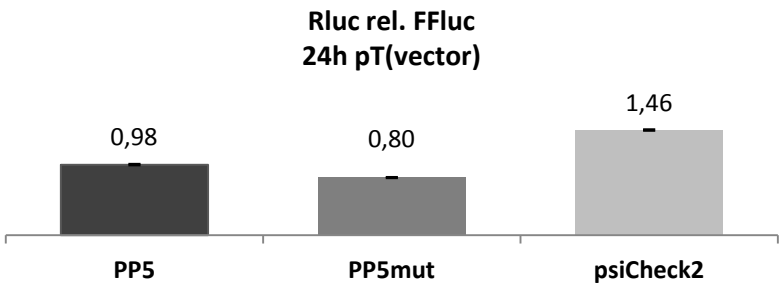

Figure 43 Calculated ratios of *Renilla* and Firefly luciferase signals for reporter vector constructs 24h after transfection.

4.10.3 Optimization of transfection for luciferase assay

As depicted in **Figure 41**, transfection efficiency for plasmids 24h after miRNA transfection was rather low. Therefore, we aimed to optimize the protocol and to address different parameters that might influence the assay: The optimization was performed by transfection of HDF5 with only the original vector (psiCheck2)

- we compared the transfection reagents Lipofectamine 2000 and Metafectene Pro
- we transfected HDF in for 12-well and 96-well format
- we determined at which time after transfection the assay should be performed
- and whether incubation with luciferase substrate had an effect on signal intensities

For the transfection in 96-well format we seeded three wells of HDF5 per reagent the day before and used 0.2 µg of vector DNA for Lipofectamine 2000 or 0.1 µg of vector DNA for Metafectene Pro (following manufacturer instructions). Each of the wells was harvested separately and cell lysates were transferred to the black detection-plate.

In 12-well format we transfected HDF5 with either 1.6 µg vector using Lipofectamine 2000 or 1 µg respectively using Metafectene Pro. For the luciferase assay we then harvested the cells and split the lysate of one 12-well to three 96-wells of the detection plate.

We captured luminescence 24h and 48h post transfection and at two different time points for each luciferase: once directly after the administration of substrate and secondly after 10 min incubation. To better demonstrate the data obtained, we did not calculate a ratio for the analysis but displayed the luminescence values directly.

The first readout from this experiment was that luminescence measurement should be performed rather 48h than 24h after vector transfection, because the signal intensities almost doubled for most of the samples (**Figures 44 and 45**).

The difference in mean standard error between the 12-well and 96-well approach can be explained by the fact that in the 12-well format we did technical replicates of the luciferase detection (one 12-well was transfected and harvested for triplicate measurement) whereas we monitored biological replicates in the 96-well format (each one of three 96-wells was transfected, harvested and measured for luminescence). Interestingly, the variation in samples harvested 24h after 96-well transfection with Lipofectamine (**Figure 45, F,H**) was rather small whereas samples lyzed 48h post transfection did not give uniform signals.

Further, we saw that incubation after adding the luciferase substrate impaired the signal intensity, which seemed more pronounced for the *Renilla* luciferase (**Figure 44, C,D**), indicating that its activity might be less stable.

Upon comparison of the transfection reagents we observed that the luminescence after 24h was lower in Metafectene Pro transfected cells than for Lipofectamine 2000 transfected ones (**Figure 45, A,B**). This could be explained by the fact that we transfected 1µg of vector DNA and 1.6 µg respectively. However after 48h, the values in these two transfection set-ups are very similar for Firefly luciferase which could be an indication for an impact of the transfection reagent on cellular growth behavior (**Fig. 44, A, B**).

A fact that – regarding the applicability for a reporter gene assay – worried us, was that we generally saw big variations in the expression of the luciferases for the two transfection reagents:

In **Figure 44, A** (48h, 0min incubation of substrate) we got a signal of about 820 for Firefly luciferase in Metafectene Pro and of approximately 785 in Lipofectamine transfected cells (**Figure 44, B**). When we compared the corresponding *Renilla* signal intensities we detected ~850 for Metafectene Pro (**Fig. 44, C**) and ~1275 for Lipofectamine. In this case, the signal ratios (Rluc/FFluc) for the same vector, transfected with two different transfection reagents, vary between 1,03 and 1,62 – implying that the transfection reagent alone could account for a more than 60% difference.

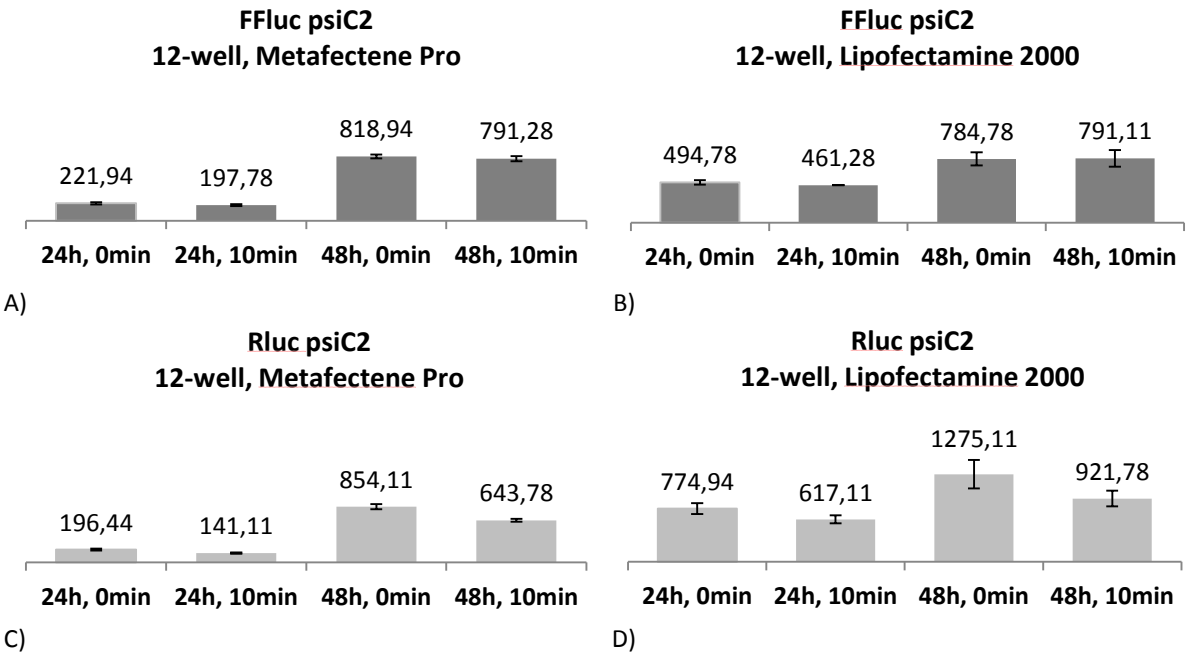

Figure 44 Raw signals of Firefly (FFluc) and *Renilla* (Rluc) luciferase for psiCheck2 (psiC2), 24h/48h after transfection with either Metafectene Pro or Lipofectamine 2000 in 12-well format. Measurement of the (technical!) sample triplicates was either done directly (0min) or after 10min of incubation.

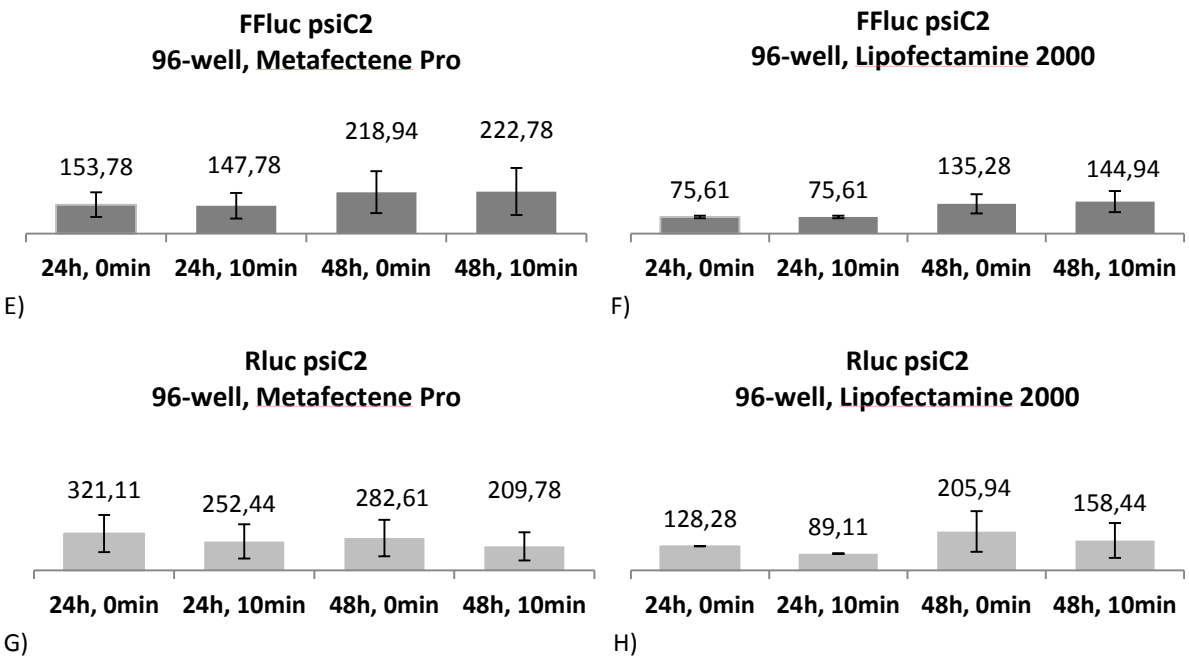

Figure 45 Raw signals of Firefly (FFFluc) and *Renilla* (Rluc) luciferase for psiCheck2 (psiC2), 24h/48h after transfection with either Metafectene Pro or Lipofectamine 2000. Measurement of the samples (biological triplicates!) was either done directly (0min) or after 10min of incubation.

4.10.4 Co-transfection of miRNA and vector

Knowing that consecutive lipofections within a short time period put a lot of strain on the cells and might impair reporter gene expression, we decided to test co-transfection of vector and miRNA using the HiPerFect system as an alternative.

Therefore we transfected HDF5 in 12-well format (preseeded 2 x 10^5 cells/well) with 30 nM miRNA-663 and 1µg plasmid DNA and captured luminescence 24h afterwards.

As can be seen in **Figure 46**, the ratios of *Renilla* and Firefly luciferase were fairly equal for the original plasmid and the construct carrying the 3'UTR of PP5 with supposed miRNA-663 binding sites. Only in the mutated version of this vector, the signal for *Renilla* luciferase was diminished - by more than 15% - as compared to the non-targeting control.

The average signal intensities in this experiment were about 3520 for FFluc and 2200 for Rluc.

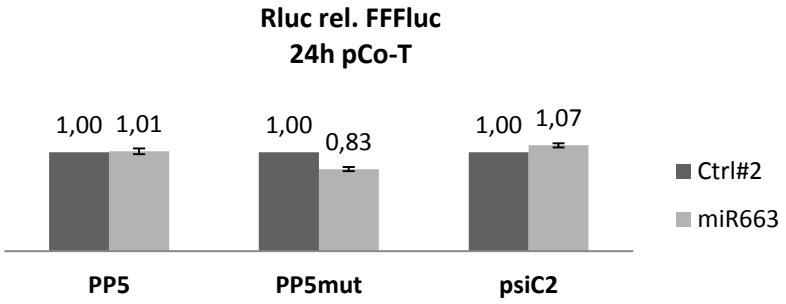

Figure 46 Calculated ratios of *Renilla* and Firefly luciferase signals 24h after co-transfection of vector constructs and 30nM miR-663, relative to miR Ctrl#2.

4.10.5 Reporter gene assay in HeLa cells

We wanted to rule out that the variations in the luciferase assay were due to the cellular background of HDF5 and inquired, whether we could reduce variability by switching to a different cell system: we chose to use HeLa cells, a commonly used immortalized human cell line, and transfected them in 96-well and 24-well format.

For experiments performed in the 96-well format, we reversely transfected 6 x 10^3 cells per well with 10 nM miRNA-663 (and control) using SiPort Neo FX. On the following day, we transfected them with the vector constructs (0.1 µg DNA per well) using transfection reagent Metafectene Pro and assayed luciferase 48h afterwards.

In the 24-well format, we started off by preseeding HeLa 1:2 and delivered the vector DNA (0.5 µg) on the next day using Metafectene Pro. 24h later, we harvested the cells and transfected 6 x 10^3 again with 10 nM miRNA. On the following day we assayed luminescence.

However, also in this experimental setup luciferase signals we obtained were not conclusive:

Figure 47 shows the luminescence ratios for reporter vector constructs expected to be regulated by miRNA-663, normalized to the non-targeting control, for the 96-well set: while the original vector (psiCheck2), 48h post transfection, showed an equal expression of both luciferases, the constructs with the native and mutated version of PP5 3'UTR indicated an increase of about 30% in *Renilla* signal, 72h after the miRNA transfection.

In **Figure 48**, the ratios for luminescence in the 24-well format are depicted: we confirmed, that performing the vector transfection on a larger scale and distributing the transfected cells for further proceedings, helps to decrease signal variation. In this experiment both the original vector as well as the mutated 3'UTR of PP5 express almost equal amounts of both luciferases, whereas the signal ratio in the construct with wild-type 3'UTR was slightly decreased. However, a clear difference indicating a regulation by miR-663 could not be observed.

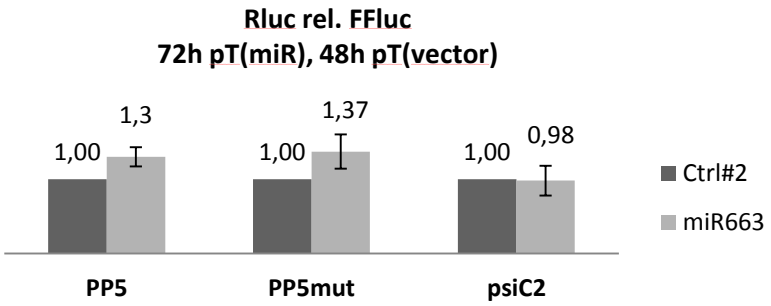

Figure 47 Calculated ratios of *Renilla* and Firefly luciferase signals 72h after transfection of 30nM miR-663 (relative to miR Ctrl#2) and 48h after transfection of vector constructs to HeLa cells (96-well).

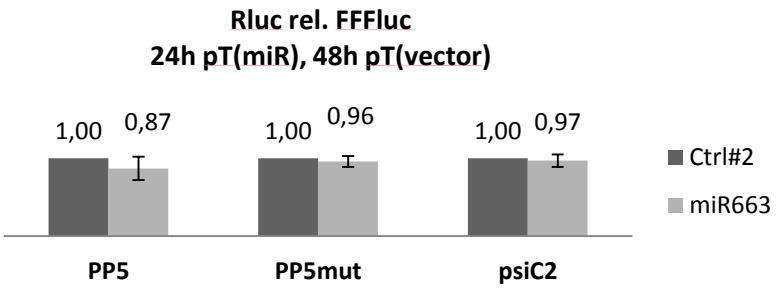

Figure 48 Calculated ratios of *Renilla* and Firefly luciferase signals 24h after transfection of 30nM miR-663 (relative to miR Ctrl#2) and 48h after transfection of vector constructs to HeLa cells (24-well).

5 DISCUSSION

Cellular senescence marks the end of a cell's replicative lifespan and is a consequence of many factors including telomere shortening, accumulation of DNA damage, oncogene activation and cellular stress levels (Campisi, 2005; Kenyon, 2010)**.** Replicative or damage induced senescence have been proposed to be important mechanisms to prevent cancer development and indeed a lot of pathways that establish the senescent phenotype, are suppressed in tumor formation. (Hanahan and Weinberg, 2000)**.**

MiRNAs – as flexible posttranscriptional regulators - have been found to play an important role in the orchestration of cellular as well as organismal aging and were associated with all the major pathways that determine cellular senescence - recently reviewed by Smith-Vikos and Slack (2012).

Precedent microarray analysis by Harald Kühnel on differentially expressed miRNAs in replicative senescent and PUVA treated human diploid fibroblasts (unpublished) showed an upregulation of miRNA-663 in both senescence scenarios compared to young, proliferating cells.

We performed a bioinformatical target prediction and found three possible binding sites for miR-663 within the 3'UTR of cell cycle phosphatase PP5. This ubiquitous protein plays an important role in the regulation of signaling cascades in proliferation, stress response, senescence and apoptosis (Golden et al., 2008a). We therefore considered it a promising and interesting candidate to be subjected to regulation by miR-663.

For evaluation of the micro-array results, we conducted qPCR analysis following Reverse transcription (see Materials and methods) and detected a more than tenfold increase in miRNA-663 abundance in senescent HDFs compared to young ones, in accordance with the screening results by Marasa et al. (2010). Levels of PP5 mRNA were about 20% lower in senescent cells.

5.1 Overexpression of miR-663

To inquire in what way overexpression of miRNA-663 affects young, proliferating cells, we transfected HDF5 with a pre-miRNA-663 resulting in a very strong increase after 24h that gradually declines with time (**Figure 17**). When we assessed mRNA and protein levels of PP5 during this time-course experiment, we found that PP5 mRNA expression is induced (about 60%) 24h post transfection and declines to the level of the mock transfected control 48h and 72h afterwards (**Figure 18**). The amount of PP5 protein however, was 24h after miR-663 transfection almost unaffected, but decreased to about 80% on the third day.

Since we saw that the fold induction during senescence is much lower than the one we achieved in our overexpression experiments, we titrated the level of miR-663 from 30nM to 1nM. A dose dependent effect of pre-miR-663 transfection was found on the levels of miRNA-663 expression (**Figure 21**), which was not reflected by the abundance of PP5 mRNA: qPCR results showed a similar fold change for miR-663 upon transfection of 1nM and 3nM whereas the corresponding levels of PP5 mRNA showed a reduction of 50% for 1nM and an induction to 200% for 3nM. Concentrations of 10nM and 30nM hardly influenced the mRNA levels of PP5 (**Figure 22**).

We decided then to inquire on the effects of prolonged miR-663 overexpression and conducted three transfections in 72h intervals. In addition to PP5 levels we also monitored p21 mRNA expression, since this cyclin dependent kinase inhibitor- as a transcriptional target of p53 – might be used as an indicator for the effect on proliferative capacity of the transfected cells (Sherr and Roberts, 1999).

The PP5 mRNA of HDFs transfected with miR-663, 72h after the first transfection (**Figure 24**) showed a more than 30% reduction, almost no change after the second transfection and a 25% reduction 72h after the last one. Western blot analysis of PP5 protein indicated a decrease that between 25% and 40% (**Figure 27**).

The effect of miR-663 overexpression on p21 mRNA levels was different to what we expected: according to our working hypothesis (**Figure 4**) a downregulation of PP5 would lead to accumulation of phosphorylated p53, which can then activate p21 transcription. Contrarily, miR-663 caused a reduction of almost 50% in p21 mRNA, even when the levels of PP5 were hardly diminished (**Figure 25, T2**) and 72h after the first and third miR-663 transfection (**Figure 25, T1** and **T3**) a decrease of about 30% was observed. A very recent report by **Yi et al. (2012)** showed that miR-663 directly targets p21 in nasopharyngeal cancer cells, which could explain the indirect correlation between miR-663 and p21 mRNA levels in we saw in HDFs.

To better study the effects of prolonged elevated levels of miR-663, the application of a stable expression vector should be considered over repeated transient transfections, since Fiszer-Kierzkowska et al. (2011) reported, that liposome based transfection interferes with stress signaling and alters transcription of stress related genes.

5.2 Oxidative stress: H_2O_2 treatment

We treated HDF5 with a sublethal dose (100 µM) of H_2O_2 to induce a p53 mediated stress response (Chen and Ames, 1994) and determined miR-663, PP5 mRNA and p21 mRNA levels by qPCR on three timepoints after the exposure:

After an initial decrease of miR-663 and PP5 mRNA (4h recovery) are both upregulated 24h following the treatment, then after 48h, their level equally drops (**Figure 28-29**). p21 mRNA levels increased almost fourfold after 4h recovery from H_2O_2 treatment and peaked 24h afterwards (more than 8 fold induction) dropping to a twofold upregulation after 48h **(Figure 30).** This shows, that the H_2O_2 treatment worked to induce p21transcription but a clear correlation to PP5 could not be observed. Possibly a larger timeframe with shorter intervals could help to elucidate the timely course of events and protein analysis would give important insights on the actual abundance of named players and p53 phosphorylation status.

5.3 Downregulation of PP5 via siRNA

In order to see whether the possibly miR-663 mediated decrease in PP5 levels in senescent cells may actually contribute to the senescent phenotype or is a mere consequence of it, we transfected young, proliferating HDF5 with a siRNA targeting PP5. siRNAs are also part of the RNAi mediated gene regulation and target genes very specifically (Elbashir et al., 2001). We saw a strong downregulation of PP5 mRNA levels (more than 80%), indicating the efficiency of RNAi (**Figure 32**)**.** We were surprised to see that 24h after the transfection of the siRNA targeting PP5 also the mRNA levels of p21 were decreased (**Figure 33**), as it was shown that a knockdown of PP5 lead to accumulation of phosphorylated $p53^{Ser15}$ and induced p21 transcription (Urban et al., 2003).

5.4 Proliferation assay

The BrdU assay for monitoring cell proliferation in miR-663 and siRNA targeting PP5 transfected HDF did not show any clear indication for an influence of either small RNAs on cell cycle progression (**Figure 34 and 35**). This was surprising, since the overexpression of miR-663 had been shown to have a strong positive impact on the proliferation of nasopharyngeal cancer cells (Yi et al., 2012)and lung cancer cells (Liu et al., 2011)**,** as well as it potently inhibits growth in gastric cancer cells (Pan et al., 2010).

Based on the findings in this experiment, the action of miRNA-663 alone is not sufficient to impact the growth behavior of normally replicating HDFs.

5.5 Reporter gene assay

We constructed a vector based on the dual luciferase reporter psiCheck2 containing 485bp of the 3'UTR of PP5 in order to assess the effect of this region on the expression of *Renilla* luciferase (see Appendix). Using a site directed mutagenesis approach we also created a mutant form in which the potential miR-663 binding sites were altered to prevent an interaction with the miRNA seed region.

For the first application we used transfected HDF5 with 30nM miR-663 (and respective control) and three constructs: the original vector (psiCheck2), psiCheck2 with the 3'UTR of PP5 and its mutated form. When we calculated the ratios relative to the mock control, we saw that miR-663 reduced *Renilla* luciferase expression about 20%, similarly in all the constructs(**Figure 42**).

In a next experiment we assessed the potential influence of the basal HDF5 miRNA environment on the reporter gene expression and found that *Renilla* luciferase was almost 1,5 fold increased – relative to Firefly luciferase – in the original vector (**Figure 43**). We also saw, that in the construct carrying the region of interest, both luciferases were expressed equally, indicating the possibility of RNAi. However, due to the fact that *Renilla* luciferase expression in the mutant was 20% lower than in the wildtype 3'UTR, we could not attribute this effect to action of miR-663.

We then tried to optimize the assay by applying different transfection reagents and parameters, altering harvesting time points and target cells (see **Figures 44-48**): we found that

- the luciferase signals were stronger 48h after vector transfection
- a 10min incubation of the substrate was not beneficial for the measurement (since *Renilla* luciferase signal seemed to decline over 10min, while Firefly luminescence stayed similar thus shifting the ratio with time; **Figure 44**)
- transfection on a larger scale (12-well versus 96-well) helped to restrict signal variations by measuring technical rather than biological replicates
- transfection reagents had a strong influence on the signal ratio obtained from the original vector: *Renilla* luciferase expression ranged from about 100% of Firefly luciferase - in Metafectene Pro transfected – to 162% of Firefly luciferase in Lipofectamine 2000 transfected cells (**Figure 44**); Co-transfection with HiPerfect showed almost equal expression of both luciferases (**Figure 46**)

Summarized, in the experiments conducted, the parameters and experimental setup seemed to have a bigger influence on the *Renilla* luciferase expression than the transfected miRNA-663.

To improve the validity of the assay, an increase of the miRNA concentration of could be considered: although we consistently achieved a strong induction using 30nM of premiR-663 in our experiments on miR-overexpression, Yi et al. (2012) applied 20µM of miR-663 to study impact on the luciferase expression in a psiCheck2 vector carrying the 3'UTR of p21. In another luciferase reporter assay on the action of miR-663, 400 ng of vector encoding the two luciferases were used per 1000ng of miR-663 expression vector (Marques et al., 2011).

In both of the above mentioned experiments from literature, the effect of miR-663 on the luciferase expression could be completely abolished in the mutated construct. Since we had verified the success of the site directed mutagenesis by sequencing we became interested in other miRNAs potentially targeting the 3'UTR of PP5.

Using the online tool DIANA - microT v3.0 (Maragkakis et al., 2009), we found two more miRNAs (miR-137 and miR-524-5p) possibly targeting PP5 and a fourth potential target site of miRNA-663 (on position 274-302) that had escaped the previous target prediction, probably because of a mismatch in the seed region (indicated by red letter, **Figure 49**). By additional site directed mutagenesis of the fourth potential binding site, the possibility could be eliminated, that the *Renilla* luciferase downregulation we saw in the mutated construct (**Figure 42, 43, 46)** was a consequence of enhanced miR-663 targeting to the fourth binding site.

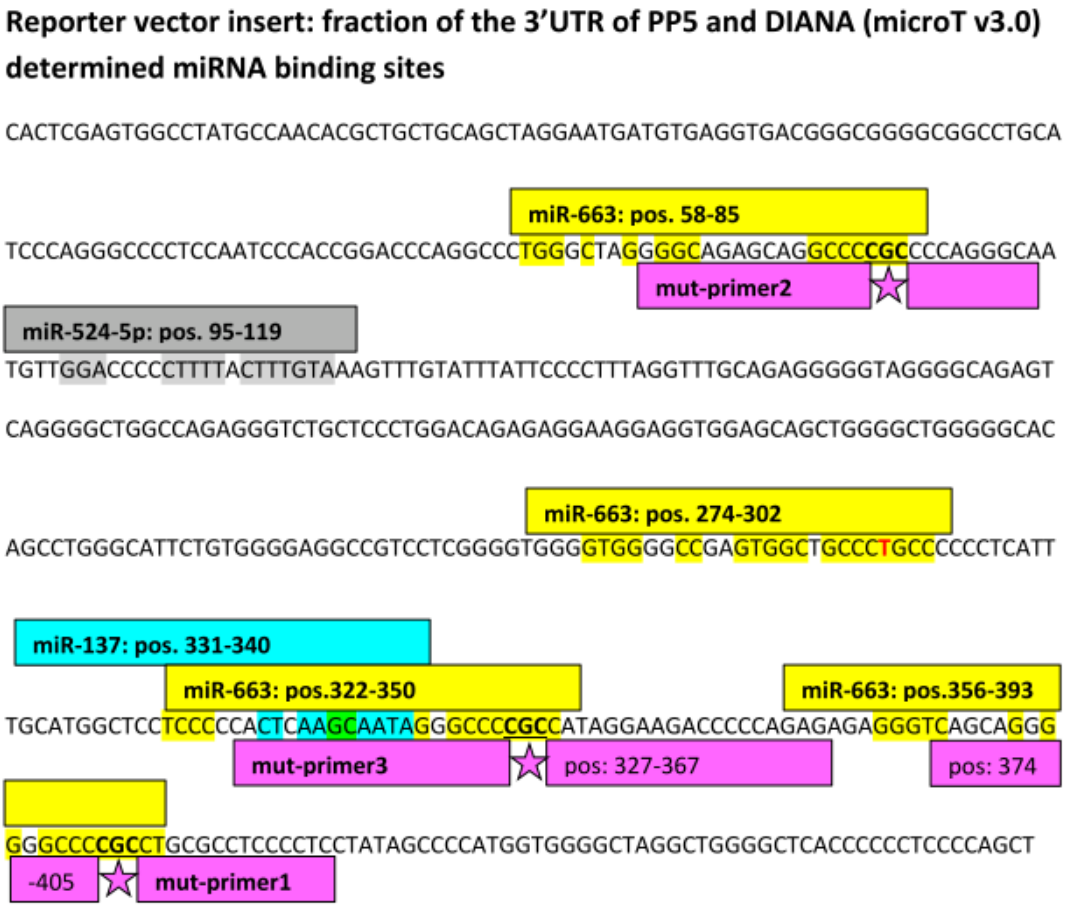

Figure 49 Overview on the predicted miRNA binding sites on the 3'UTR of PP5 as determined by DIANA - microT v3.0 (Maragkakis et al., 2009). Potential miR-663 binding regions are highlighted in yellow, site directed mutagenesis primer in pink boxes with star indicating mismatch from CGC to TAT. Other miRNAs that were suggested by DIANA to bind the 3'UTR are indicated by blue and grey boxes respectively.

5.6 Summary

The upregulation of miRNA-663 in DNA damage induced and replicative senescence in human diploid fibroblasts is a confirmed observation (Maes et al., 2009; Marasa et al., 2010) and its influence on cellular proliferation has been affirmed by several studies on cancer cells. The fact that miR-663 has been described – dependent on cell type - both as tumor suppressor (Pan et al., 2010, 2011; Tili et al., 2010b) as well as a tumor promoter (Liu et al., 2011) illustrates the complexity of its proliferative signal regulations.

Bioinformatical target search for miR-663 predicted three, to possibly four, binding sites in protein phosphatase 5, leading to our working hypothesis: miRNA-663 upregulation results in lower levels of PP5, which leads to accumulation of phosphorylated p53 and ultimately G1 cell cycle arrest in senescent cells due to enhanced transcription of p21.

Thus we wanted to verify, if PP5 is indeed a target of miRNA-663 and whether we could induce a senescence-like phenotype by overexpression of miR-663 in young HDF or at least diminished proliferation.

Due to the many inconsistencies the results of luciferase assay did not provide any conclusive data for a direct interaction between the 3'UTR of PP5 and miRNA-663. On the contrary, the experimental parameters seemed to have a bigger influence on luciferase expression than the actual transfection of miRNA-663.

MiRNA-663 overexpression in young, proliferating HDF showed a clear correlation between miR-663 and the amount of PP5 protein levels that did not necessarily correspond with PP5 mRNA levels. However, we could not observe a similar correlation between PP5 mRNA levels and miRNA-663 fold changes. Yet one has to consider, that the effect of a miRNA – as translational repressor - can be observed more frequently on protein rather than mRNA level. In addition, it was recently shown, that miR-663 also regulates the activity of transcription factor AP-1 by directly targeting its components JunB and JunD (Tili et al., 2010a). AP-1 is widely involved in the regulation of genes for proliferation, apoptosis, differentiation and inflammation (Shaulian, 2010) and could potentially also influence PP5 transcription.

Upon knock down of PP5 using siRNA or prolonged overexpression of miR-663 we saw that decreased levels of PP5 mRNA or protein, didn't conditionally result in an increase in p21 mRNA (as suggested by our hypothesis) but showed a similar downregulation.

To determine whether this is due to lack of p53 activation or consequence of p53 independent p21 transcription (Gartel and Radhakrishnan, 2005) the phosphorylation status of p53 in our experiments

needs to be assessed. Yet there is still the possibility that in HDF5 – similar to nasopharyngeal cells (Yi et al., 2012) - also a direct interaction of p21 with miR-663 causes the reduction of p21 mRNA.

In young HDF5, we could not see that overexpression of miR-663 or siRNA knockdown of PP5 alone was sufficient to affect proliferation as assessed by BrdU incorporation. According to our model, the induction of DNA damage (consequently activation of p53) might be required in addition to see an effect of PP5 downregulation on cell cycle progression.

Following treatment with sublethal doses of hydrogen peroxide to induce DNA damage (Chen and Ames, 1994) we found that the expression of miRNA-663 to be very variable: after an initial downregulation (0.5 fold) it was slightly upregulated 24h after treatment (1.3 fold) and then downregulated (0.4 fold) again.

This could indicate a possible involvement in fine tuning of repair programs and stress signal regulation which should be further investigated by including more time points and a longer experimental time frame. Also the characterization of replicative capacity in treated cells would help to clarify the role of miRNA-663 in these processes.

Still we find the idea that miR-663 is involved in the cellular response to stress very appealing. Recent data from literature clearly indicates a role of miR-663 in cellular proliferation and PP5 is an established regulator of stress induced signaling networks and cancer (Golden et al., 2008).

Our data currently indicates that PP5 is not directly regulated by miR-663, however some of our observations are still in line with at least an indirect regulation for example via JunB and JunD (Tili et al., 2010a).

Finally, our results showed that especially when working with normal human cells, investigating the delicately balanced response to stress and sub-lethal damage requires a very sophisticated experimental set-up.

6 ACKNOWLEDGEMENTS

I want to express my honest gratitude to all the group members of Grillari labs at the University of Natural Resources and Life Sciences, Vienna (BOKU) for the constructive and motivational atmosphere and the kind helpfulness that made the practical work on this thesis a wonderful experience. In particular I want to thank Dr. Johannes Grillari for being an inspirational and enthusiastic group leader and my dedicated supervisor Dr. Matthias Wieser, who both supported and challenged me with patience and great scientific expertise.

7 REFERENCES

Alcorta, D.A., Xiong, Y., Phelps, D., Hannon, G., Beach, D., and Barrett, J.C. (1996). Involvement of the cyclin-dependent kinase inhibitor p16 (INK4a) in replicative senescence of normal human fibroblasts. PNAS *93*, 13742–13747.

Bartel, D.P. (2004). MicroRNAs: genomics, biogenesis, mechanism, and function. Cell *116*, 281–297.

Berezikov, E., Chung, W.-J., Willis, J., Cuppen, E., and Lai, E.C. (2007). Mammalian Mirtron Genes. Molecular Cell *28*, 328–336.

Boehm, M., and Slack, F. (2005). A developmental timing microRNA and its target regulate life span in C. elegans. Science *310*, 1954–1957.

Campisi, J. (2005). Senescent Cells, Tumor Suppression, and Organismal Aging: Good Citizens, Bad Neighbors. Cell *120*, 513–522.

Chen, Q., and Ames, B.N. (1994). Senescence-like growth arrest induced by hydrogen peroxide in human diploid fibroblast F65 cells. Proc Natl Acad Sci U S A *91*, 4130–4134.

Cimino, G.D., Gamper, H.B., Isaacs, S.T., and Hearst, J.E. (1985). Psoralens as photoactive probes of nucleic acid structure and function: organic chemistry, photochemistry, and biochemistry. Annu. Rev. Biochem. *54*, 1151–1193.

Colgin, L.M., and Reddel, R.R. (1999). Telomere maintenance mechanisms and cellular immortalization. Current Opinion in Genetics & Development *9*, 97–103.

Derheimer, F.A., Hicks, J.K., Paulsen, M.T., Canman, C.E., and Ljungman, M. (2009). Psoralen-Induced DNA Interstrand Cross-Links Block Transcription and Induce p53 in an Ataxia-Telangiectasia and Rad3-Related-Dependent Manner. Mol Pharmacol *75*, 599–607.

Efeyan, A., and Serrano, M. (2007). p53: guardian of the genome and policeman of the oncogenes. Cell Cycle *6*, 1006–1010.

Elbashir, S.M., Lendeckel, W., and Tuschl, T. (2001). RNA interference is mediated by 21- and 22-nucleotide RNAs. Genes Dev. *15*, 188–200.

Eulalio, A., Huntzinger, E., and Izaurralde, E. (2008). GW182 interaction with Argonaute is essential for miRNA-mediated translational repression and mRNA decay. Nature Structural & Molecular Biology *15*, 346–353.

Fabian, M.R., and Sonenberg, N. (2012). The mechanics of miRNA-mediated gene silencing: a look under the hood of miRISC. Nature Structural & Molecular Biology *19*, 586–593.

Fagagna, F. d'Adda di (2008). Living on a break: cellular senescence as a DNA-damage response. Nature Reviews Cancer *8*, 512–522.

Fagagna, F. d'Adda di, Reaper, P.M., Clay-Farrace, L., Fiegler, H., Carr, P., Zglinicki, T. von, Saretzki, G., Carter, N.P., and Jackson, S.P. (2003). A DNA damage checkpoint response in telomere-initiated senescence. Nature *426*, 194–198.

Gartel, A.L., and Radhakrishnan, S.K. (2005). Lost in Transcription: p21 Repression, Mechanisms, and Consequences. Cancer Res *65*, 3980–3985.

Gems, D., and Partridge, L. (2012). Genetics of Longevity in Model Organisms: Debates and Paradigm Shifts. Annu. Rev. Physiol.

Golden, T., Swingle, M., and Honkanen, R.E. (2008). Role of serine threonine protein phosphatase type 5 (PP5) in the regulation of stress induced signaling networks and cancer. Cancer Metastasis Rev *27*, 169–178.

Gregory, R.I., Chendrimada, T.P., and Shiekhattar, R. (2006). MicroRNA Biogenesis: Isolation and Characterization of the Microprocessor Complex. In MicroRNA Protocols, S.-Y. Ying, ed. (Humana Press), pp. 33–47.

Griffiths-Jones, S., Saini, H.K., Van Dongen, S., and Enright, A.J. (2008). miRBase: tools for microRNA genomics. Nucleic Acids Res. *36*, D154–158.

Grillari, J., Hackl, M., and Grillari-Voglauer, R. (2010). miR-17-92 cluster: ups and downs in cancer and aging. Biogerontology *11*, 501–506.

Hanahan, D., and Weinberg, R. (2000). The Hallmarks of Cancer. Cell *100*, 57–70.

Hayflick, L. (1965). The limited in vitro lifetime of human diploid cell strains. Experimental Cell Research *37*, 614–636.

Henson, J., D., Neumann, A., A., Yeager, T., R., and Reddel, R., R. (2002). Alternative lengthening of telomeres in mammalian cells. , Published Online: 18 January 2002; | Doi:10.1038/sj.onc.1205058 *21*.

Hinds Jr., T.D., and Sánchez, E.R. (2008). Protein phosphatase 5. The International Journal of Biochemistry & Cell Biology *40*, 2358–2362.

Hovest, M.G., Brüggenolte, N., Hosseini, K.S., Krieg, T., and Herrmann, G. (2006). Senescence of human fibroblasts after psoralen photoactivation is mediated by ATR kinase and persistent DNA damage foci at telomeres. Mol. Biol. Cell *17*, 1758–1767.

Jacobs, J.J.L., and Lange, T. de (2005). p16INK4a as a Second Effector of the Telomere Damage Pathway. Cell Cycle *4*, 1364–1368.

Kato, M., Chen, X., Inukai, S., Zhao, H., and Slack, F.J. (2011). Age-associated changes in expression of small, noncoding RNAs, including microRNAs, in C. elegans. RNA *17*, 1804–1820.

Kenyon, C. (2005). The plasticity of aging: insights from long-lived mutants. Cell *120*, 449–460.

Kenyon, C.J. (2010). The genetics of ageing. Nature *464*, 504–512.

Krek, A., Grün, D., Poy, M.N., Wolf, R., Rosenberg, L., Epstein, E.J., MacMenamin, P., Da Piedade, I., Gunsalus, K.C., Stoffel, M., et al. (2005). Combinatorial microRNA target predictions. Nat. Genet. *37*, 495–500.

Lee, R.C., Feinbaum, R.L., and Ambros, V. (1993). The C. elegans heterochronic gene lin-4 encodes small RNAs with antisense complementarity to lin-14. Cell *75*, 843–854.

Li, G., Luna, C., Qiu, J., Epstein, D.L., and Gonzalez, P. (2009). Alterations in microRNA expression in stress-induced cellular senescence. Mech. Ageing Dev. *130*, 731–741.

Liu, N., Landreh, M., Cao, K., Abe, M., Hendriks, G.-J., Kennerdell, J.R., Zhu, Y., Wang, L.-S., and Bonini, N.M. (2012). The microRNA miR-34 modulates ageing and neurodegeneration in Drosophila. Nature *482*, 519–523.

Liu, Z.-Y., Guang-Ling, Z., Mei-Mei, W., Ya-Nan, X., and He-Qin, C. (2011). MicroRNA-663 Targets TGFB1 and Regulates Lung Cancer Proliferation. Asian Pacific Journal of Cancer Prevention *12*, 2819–2823.

Maes, O.C., Sarojini, H., and Wang, E. (2009). Stepwise up-regulation of microRNA expression levels from replicating to reversible and irreversible growth arrest states in WI-38 human fibroblasts. J. Cell. Physiol. *221*, 109–119.

Mallette, F.A., and Ferbeyre, G. (2007). The DNA damage signaling pathway connects oncogenic stress to cellular senescence. Cell Cycle *6*, 1831–1836.

Maragkakis, M., Reczko, M., Simossis, V.A., Alexiou, P., Papadopoulos, G.L., Dalamagas, T., Giannopoulos, G., Goumas, G., Koukis, E., Kourtis, K., et al. (2009). DIANA-microT web server: elucidating microRNA functions through target prediction. Nucl. Acids Res. *37*, W273–W276.

Marasa, B.S., Srikantan, S., Masuda, K., Abdelmohsen, K., Kuwano, Y., Yang, X., Martindale, J.L., Rinker-Schaeffer, C.W., and Gorospe, M. (2009). Increased MKK4 abundance with replicative senescence is linked to the joint reduction of multiple microRNAs. Sci Signal *2*, ra69.

Marasa, B.S., Srikantan, S., Martindale, J.L., Kim, M.M., Lee, E.K., Gorospe, M., and Abdelmohsen, K. (2010). MicroRNA profiling in human diploid fibroblasts uncovers miR-519 role in replicative senescence. Aging (Albany NY) *2*, 333–343.

Marques, F.Z., Campain, A.E., Tomaszewski, M., Zukowska-Szczechowska, E., Yang, Y.H.J., Charchar, F.J., and Morris, B.J. (2011). Gene expression profiling reveals renin mRNA overexpression in human hypertensive kidneys and a role for microRNAs. Hypertension *58*, 1093–1098.

Mirzayans, R., Andrais, B., Hansen, G., and Murray, D. (2012). Role of p16INK4A in Replicative Senescence and DNA Damage-Induced Premature Senescence in p53-Deficient Human Cells. Biochemistry Research International *2012*, 1–8.

Mogi, S., Butcher, C.E., and Oh, D.H. (2008). DNA polymerase η reduces the γ-H2AX response to psoralen interstrand crosslinks in human cells. Exp Cell Res *314*, 887–895.

Morison, W.L. (1999). Phototherapy and photochemotherapy: An update. Seminars in Cutaneous Medicine and Surgery *18*, 297–306.

Mudhasani, R., Zhu, Z., Hutvagner, G., Eischen, C.M., Lyle, S., Hall, L.L., Lawrence, J.B., Imbalzano, A.N., and Jones, S.N. (2008). Loss of miRNA biogenesis induces p19Arf-p53 signaling and senescence in primary cells. J. Cell Biol. *181*, 1055–1063.

Pan, J., Hu, H., Zhou, Z., Sun, L., Peng, L., Yu, L., Sun, L., Liu, J., Yang, Z., and Ran, Y. (2010). Tumor-suppressive mir-663 gene induces mitotic catastrophe growth arrest in human gastric cancer cells. Oncol. Rep. *24*, 105–112.

Pan, J., Li, Z.W., Fang, T.Y., Jian, W., Zhuan, Z., Mei, L.X., Yan, W.S., and Jian, N. (2011). Retinoic acid induces HL-60 cell differentiation via the upregulation of miR-663. Journal of Hematology & Oncology *4*, 1–8.

Rana, T.M. (2007). Illuminating the silence: understanding the structure and function of small RNAs. Nature Reviews Molecular Cell Biology *8*, 23–36.

Romanov, V.S., Pospelov, V.A., and Pospelova, T.V. (2012). Cyclin-dependent kinase inhibitor p21Waf1: Contemporary view on its role in senescence and oncogenesis. Biochemistry Moscow *77*, 575–584.

Shaulian, E. (2010). AP-1--The Jun proteins: Oncogenes or tumor suppressors in disguise? Cell. Signal. *22*, 894–899.

Shay, J.W., and Wright, W.E. (2005). Senescence and immortalization: role of telomeres and telomerase. Carcinogenesis *26*, 867–874.

Sherr, C.J., and Roberts, J.M. (1999). CDK inhibitors: positive and negative regulators of G1-phase progression. Genes Dev. *13*, 1501–1512.

Smith-Vikos, T., and Slack, F.J. (2012). MicroRNAs and their roles in aging. Journal of Cell Science *125*, 7–17.

Stein, G.H., Drullinger, L.F., Soulard, A., and Dulić, V. (1999). Differential roles for cyclin-dependent kinase inhibitors p21 and p16 in the mechanisms of senescence and differentiation in human fibroblasts. Mol. Cell. Biol. *19*, 2109–2117.

Tili, E., Michaille, J.-J., Adair, B., Alder, H., Limagne, E., Taccioli, C., Ferracin, M., Delmas, D., Latruffe, N., and Croce, C.M. (2010a). Resveratrol decreases the levels of miR-155 by upregulating miR-663, a microRNA targeting JunB and JunD. Carcinogenesis *31*, 1561–1566.

Tili, E., Michaille, J.-J., Alder, H., Volinia, S., Delmas, D., Latruffe, N., and Croce, C.M. (2010b). Resveratrol modulates the levels of microRNAs targeting genes encoding tumor-suppressors and effectors of TGFβ signaling pathway in SW480 cells. Biochem. Pharmacol. *80*, 2057–2065.

Ugalde, A.P., Ramsay, A.J., De la Rosa, J., Varela, I., Mariño, G., Cadiñanos, J., Lu, J., Freije, J.M., and López-Otín, C. (2011). Aging and chronic DNA damage response activate a regulatory pathway involving miR-29 and p53. EMBO J. *30*, 2219–2232.

Urban, G., Golden, T., Aragon, I.V., Cowsert, L., Cooper, S.R., Dean, N.M., and Honkanen, R.E. (2003). Identification of a functional link for the p53 tumor suppressor protein in dexamethasone-induced growth suppression. J. Biol. Chem. *278*, 9747–9753.

Watson, J.D. (1972). Origin of concatemeric T7 DNA. Nat New Biol. *239*, 197–201.

Wlaschek, M., Ma, W., Jansen-Dürr, P., and Scharffetter-Kochanek, K. (2003). Photoaging as a consequence of natural and therapeutic ultraviolet irradiation--studies on PUVA-induced senescence-like growth arrest of human dermal fibroblasts. Exp. Gerontol. *38*, 1265–1270.

Yamakuchi, M., and Lowenstein, C.J. (2009). MiR-34, SIRT1 and p53: the feedback loop. Cell Cycle *8*, 712–715.

Yi, C., Wang, Q., Wang, L., Huang, Y., Li, L., Liu, L., Zhou, X., Xie, G., Kang, T., and Wang, H. (2012). MiR-663, a microRNA targeting p21WAF1/CIP1, promotes the proliferation and tumorigenesis of nasopharyngeal carcinoma. Oncogene.

8 APPENDIX

8.1 Materials for cloning

8.1.1 Primers

cloning_PP5_fwd; *=*Xho1* cutting site	**CAC*TCGAGTGGCCTATGCCAACACGCTGC**
cloning_PP5_rev; * = *Not1* cutting site	**GCGC*GGCCGCGGGGTGAGCCCCAGCCTAGC**
psiCheck2_sequencing_sense	**TACCTTCGGGCCAGCGACGA**
psiCheck2_sequencing_as	**GCCAGTTACCACCCGCCGAC**
PPP5C_mut primer 1	**CAGCAGGGGGGCCCTATCTGCGCCTCCCCTC**
PPP5C_mut primer 2	**GGGCAGAGCAGGCCCTATCCCAGGGCAATGTTG**
PPP5C_mut primer 3	**CACTCAAGCAATAGGGCCCTATCATAGGAAGACCCCCAGAG**

Table 22: Primers for cloning of psiCheck2_3'UTR_PP5 and site directed mutagenesis

8.1.2 Polymerases

Taq DNA polymerase – Biotools

8.1.3 Restriction Endonucleases + Ligases

Xho1 - New England Biolabs

Not1 - New England Biolabs

Buffer 3 – New England Biolabs

T4 Ligase - New England Biolabs

T4 Ligase buffer - New England Biolabs

CIP (Alkaline Phosphatase from Calf intestine) – New England Biolabs

8.1.4 Electroporation + Plating

BTX-630B Safety Stand - Electroporator

Liquid LB (100 µg/ml Ampicillin) medium (autoclaved); pH 7.5

LB medium liquid (1000ml)	
NaCl	10 g
Bacto tryptone	10 g
Bacto yeast extract	5 g

Table 23 LB medium components

LB agar plates (100 µg/ml Ampicillin); liquid LB + 1.5% agar

SOC medium (autoclaved)

SOC medium (1000ml)	
5M NaCl	2 ml
1M KCl	2.5 ml
1M $MgCl_2$	10 ml
1M $MgSO_4$	10 ml
1M glucose	20 ml
Bacto tryptone	20 g
Bacto yeast extract	5 g

Table 24 components of SOC medium

8.1.5 Gel electrophoresis and DNA purification

TAE buffer: 40 mM Tris-acetate, 1mM EDTA

BioRad Gel chambers

Wizard® SV Gel and PCR Clean-Up System – Promega

Nanodrop ND-1000 – Peqlab

8.1.6 Plasmid preparation

EndoFree Plasmid Maxi Kit - Quiagen

Wizard® Plus SV Minipreps DNA Purification System – Promega

8.1.7 QuickChange ® Multi Site-Directed Mutagenesis

QuickChange ® Mulit Site-Directed Mutagenesis Kit - Stratagene

QuikChange® Multi enzyme blend (2.5 U/µl) - Stratagene

10× QuikChange®Multi reaction buffer - Stratagene

Dpn I restriction enzyme (10 U/µl) 300 U - Stratagene

QuikChange® Multi control template (50 ng/ µl) - Stratagene

QuikChange® Multi control primer mix (100 ng/µl of each of three primers) - Stratagene

XL10-Gold®ultracompetent cells[3] - Stratagene

XL10-Gold®β-mercaptoethanol mix - Stratagene

pUC18 control plasmid (0.1 ng/µl in TE buffer) - Stratagene

5-Bromo-4-chloro-3-indoyl-β-D-galactopyranoside (X-gal)

Isopropyl-1-thio-β-D-galactopyranoside (IPTG)

[3] Genotype: Tet^R Δ(*mcrA*) 183 Δ(*mcrCB-hsdSMR-mrr*) 173 *endA1 supE44 thi-1 recA1 gyrA96 relA1 lac* Hte [F′ *proAB* $lacI^qZ\Delta M15$ Tn10 (Tet^R) Amy Cam^R

NZY-Broth (1000ml) pH: 7,5	
NaCl	5 g
$MgSO_4*7H_2O$	2 g
Bacto yeast extract	5 g
NZ amine (casein hydrolysate)	10 g
ddH_2O	to 1000 ml

Table 25 medium components for NZY-Broth

8.2 Materials for cell culture

8.2.1 Cultivation

HDF 5 full medium components:	
DMEM / Ham's F12	1:1
l-Gln	4 mM
FCS	10 %

Solutions	25cm²	75cm²	125cm²
PBS for washing	~4 ml	~8 ml	~15 ml
Trypsine 0,1%	0.5 ml	1 ml	2 ml
Medium	6 ml	15 ml	35 ml

Table 26 Formula of HDF5 medium and volumes used for HDF5 maintenance

Dulbecco's PBS 1x w/o Ca^{2+}, Mg^{2+} - PAA

Dulbecco's modified Eagle medium (DMEM) - Biochrom

Ham's F12 medium - Biochrom

L-Gln - Sigma

FCS – PAA

0.1 % trypsine - Invitrogen

Hera cell Heraeus incubator - Thermo Electron corp.

Cellstar cell culture flasks (25cm², 75cm² + 125cm²) – Greiner bio-one

8.2.2 Transfection

Trypane-blue - Sigma

Cell counting chamber - Bürker Türk

Optimem – Gibco

HBS buffer – 150 mM NaCl,20mM Hepes, ph 7.4

SiPort Neo FX – Applied Biosystems

Metafectene Pro – Biontex Laboratories

Lipofectamine 2000 – Invitrogen

HiPerfect Transfection Reagent – Quiagen

DharmaFECT ® Duo Transfection Reagent – Thermo Scientific

pmaxGFP – Lonza

psiCheck2™ - Invitrogen

Pre-miR-663 – Ambion

Pre-miR-Ctrl#2 – Ambion

Pre-miR-fam– Ambion

Pre-Cy3miR– Ambion

siGLO green – Dharmacon

siRNA tPP5 (ISIS 15534) – Dharmacon

8.2.3 Harvesting reagents

TRIzol® Reagent -. Invitrogen

Nuclear Extract Buffer:

Nuclear Extract Buffer	
Tris base	50mM
NaCl	0,5M
NaDeoxicholate	1%
SDS	0,1%
EDTA	2mM
NP40 substitute	1%
Complete protease inhibitor	1 pellet

Table 27 Reagent list for Nuclear Extract Buffer

8.3 Materials: sample preparation + analysis

8.3.1 Protein analysis

BCA Protein Assay Reagent – Pierce

NuPAGE™ – Invitrogen

ProtoGel (30%) Acrylamide and Bisacrylamide, 37.5 : 1– National Diagnostics

Resolving gel buffer (4x)	
Tris base	91 g
H_2O	500ml
Adjust pH to 8.8 with HCl	

Stacking gel premix (40ml)	
Resolving gel buffer (4x)	10 ml
Acrylamide/Bisacrylamide (37.5:1)	5 ml
H_2O	24,2 ml
SDS (20%)	0.8 ml

Table 28 Preparation of buffers for Western blotting

4x SDS Loading Dye

PAA gel apperature - Hoefer

SeeBlue® Plus2 pre stained protein standard – Invitrogen

Roti ®PVDF membrane – Roth

TPBS (blocking buffer): PBS + 1:1000 Tween 20, pH 7.4

Milk powder

Mouse anti-PP5 antibody – BD Transduction Laboratories

Alexa Fluor 594 goat anti-mouse IgG

Rabbit anti-GAPDH antibody –Sigma

Alexa Fluor 488 anti-rabbit IgG

α-mouse-peroxidase antibody - Sigma

Pierce ® ECL Western Blotting – Thermo scientific

Lumi-ImagerTM F1 Boehringer

IKA-Vibrax Shaker – VXR

Transblot SD Elektroblotter– Biorad

Odyssey® Infrared Imaging System – Li-Cor

8.3.2 RNA analysis

RNase Zap ®wipes - Invitrogen

Chloroform

Isopropanol

70 % Ethanol

GlycoBlue™ - Ambion

QIAshredder columns – Quiagen

Polystyrene tubes, Sarstedt tubes

DyNAmo™ cDNA Synthesis Kit - Finnzymes

TB Thermocycler Biotron - Biometra

NCode™ miRNA First-Strand cDNA Synthesis and qRT-PCR Kit – Invitrogen

8.3.3 qPCR

SensiMix™ SYBR & Fluorescein Kit - Bioline

RG-6000 Rotorgene – Rcorbett research Quiagen

8.3.4 qPCR primers

GAPDH_RTneu1_sense	**CGACCACTTTGTCAAGCTCA**
GAPDH_RTneu1_as	**TGTGAGGAGGGGAGATTCAG**
PPP5C_1_fwd_RT	**GGCTGCCAGCAACATGGCAC**
PPP5C_1_rev_RT	**ACGGAGCGCTTGTGCTCGTC**
P21_RT_fwd	**GCAGGGGGCGGCCAGGGTAT**
P21_RT_rev	**GGCGGCAGACCAGCATGACAGATT**
Universal qPCR Primer for NCode™	**Oligo dT (provided with kit)**
5s_rRNA	**CAGGGTCGGGCCTGGTTAGTACTTG**
hsa-miR-663	**AGGCGGGGCGCCGCGGGAC**

Table 29 Primers used for qPCR analysis

8.3.5 BrdU assay

10mM BrdU

70% Ethanol (-20°C)

2M HCl 1% Triton

0,1M Na-Borat pH 8.5

TBS: 0.5 % Tween20, 1 % BSA in PBS

Monoclonal mouse anti-BrdU antibody - BD (CatNo 347580)

Anti-mouse FITC-conjugated antibody – Sigma (F-8264)

1mg/ml PI (Propidium Iodide)

FACSCalibur™ - Becton Dickinson

8.3.6 Luciferase assay

Synergy 2 plate reader - BioTek

Glo Lysis Buffer, 1X - Promega

Dual-Glo® Luciferase Assay System – Promega

Black 96-well plate

8.4 Vector sequence: psiCheck2_3'UTR_PPP5C

light green: *Renilla* luciferase ORF
grey: Firefly luciferase ORF
blue/red: ligation of *Xho1* and *Not1* restriction sites
yellow: amplicon of 3'UTR of PP5 PCR (cloning primers)
pink: seed region of miRNA-663; bases CGC were altered to TAT in site directed mutagenesis

AGATCTGCGCAGCACCATGGCCTGAAATAACCTCTGAAAGAGGAACTTGGTTAGGTACCTTCTGAGGCGGAAAGAACCAGCTGTGGAATGTGTG
TCAGTTAGGGTGTGGAAAGTCCCCAGGCTCCCCAGCAGGCAGAAGTATGCAAAGCATGCATCTCAATTAGTCAGCAACCAGGTGTGGAAAGTCC
CCAGGCTCCCCAGCAGGCAGAAGTATGCAAAGCATGCATCTCAATTAGTCAGCAACCATAGTCCCGCCCCTAACTCCGCCCATCCCGCCCCTAA
CTCCGCCCAGTTCCGCCCATTCTCCGCCCCATGGCTGACTAATTTTTTTTATTTATGCAGAGGCCGAGGCCGCCTCGGCCTCTGAGCTATTCCA
GAAGTAGTGAGGAGGCTTTTTTGGAGGCCTAGGCTTTTGCAAAAAGCTTGATTCTTCTGACACAACAGTCTCGAACTTAAGCTGCAGAAGTTGG
TCGTGAGGCACTGGGCAGGTAAGTATCAAGGTTACAAGACAGGTTTAAGGAGACCAATAGAAACTGGGCTTGTCGAGACAGAGAAGACTCTTGC
GTTTCTGATAGGCACCTATTGGTCTTACTGACATCCACTTTGCCTTTCTCTCCACAGGTGTCCACTCCCAGTTCAATTACAGCTCTTAAGGCTA
GAGTACTTAATACGACTCACTATAGGCTAGCCACCATGGCTTCCAAGGTGTACGACCCCGAGCAACGCAAACGCATGATCACTGGGCCTCAGTG
GTGGGCTCGCTGCAAGCAAATGAACGTGCTGGACTCCTTCATCAACTACTATGATTCCGAGAAGCACGCCGAGAACGCCGTGATTTTTCTGCAT
GGTAACGCTGCCTCCAGCTACCTGTGGAGGCACGTCGTGCCTCACATCGAGCCCGTGGCTAGATGCATCATCCCTGATCTGATCGGAATGGGTA
AGTCCGGCAAGAGCGGGAATGGCTCATATCGCCTCCTGGATCACTACAAGTACCTCACCGCTTGGTTCGAGCTGCTGAACCTTCCAAAGAAAAT
CATCTTTGTGGGCCACGACTGGGGGGCTTGTCTGGCCTTTCACTACTCCTACGAGCACCAAGACAAGATCAAGGCCATCGTCCATGCTGAGAGT
GTCGTGGACGTGATCGAGTCCTGGGACGAGTGGCCTGACATCGAGGAGGATATCGCCCTGATCAAGAGCGAAGAGGGCGAGAAAATGGTGCTTG
AGAATAACTTCTTCGTCGAGACCATGCTCCCAAGCAAGATCATGCGGAAACTGGAGCCTGAGGAGTTCGCTGCCTACCTGGAGCCATTCAAGGA
GAAGGGCGAGGTTAGACGGCCTACCCTCTCCTGGCCTCGCGAGATCCCTCTCGTTAAGGGAGGCAAGCCCGACGTCGTCCAGATTGTCCGCAAC
TACAACGCCTACCTTCGGGCCAGCGACGATCTGCCTAAGATGTTCATCGAGTCCGACCCTGGGTTCTTTTCCAACGCTATTGTCGAGGGAGCTA
AGAAGTTCCCTAACACCGAGTTCGTGAAGGTGAAGGGCCTCCACTTCAGCCAGGAGGACGCTCCAGATGAAATGGGTAAGTACATCAAGAGCTT
CGTGGAGCGCGTGCTGAAGAACGAGCAGTAATTCTAGGCGATCGCTCactcgagtggcctatgccaacacgctgctgcagctaggaatgatgtg
aggtgacgggcggggcggcctgcatcccagggcccctccaatcccaccggacccaggccctgggctaggggcagagcaggccccgccccagggc
aatgttggacccccttttactttgtaaagtttgtatttattccccctttaggtttgcagaggggggtaggggcagagtcaggggctggccagaggg
tctgctccctggacagagaggaaggaggtggagcagctggggctgggggcacagcctgggcattctgtggggaggccgtcctcggggtggggtg
gggccgagtggctgccctgccccccctcatttgcatggctcctccccccactcaagcaataggggccccgccataggaagaccccccagagagagggt
cagcaggggggccccgccctgcgcctcccctcctatagccccatggtggggctaggctggggctcaccccgcggccgcggcGGCCGCTGGCCGCAA
TAAAATATCTTTATTTTCATTACATCTGTGTGTTGGTTTTTTGTGTGAGGATCTAAATGAGTCTTCGGACCTCGCGGGGGCCGCTTAAGCGGTG
GTTAGGGTTTGTCTGACGCGGGGGGAGGGGGAAGGAACGAAACACTCTCATTCGGAGGCGGCTCGGGGTTTGGTCTTGGTGGCCACGGGCACGC
AGAAGAGCGCCGCGATCCTCTTAAGCACCCCCCCGCCCTCCGTGGAGGCGGGGGGTTTGGTCGGCGGGTGGTAACTGGCGGGCCGCTGACTCGGG
CGGGTCGCGCGCCCCAGAGTGTGACCTTTTCGGTCTGCTCGCAGACCCCCGGGCGGCGCCGCCGCGGCGGCGACGGGCTCGCTGGGTCCTAGGC
TCCATGGGGACCGTATACGTGGACAGGCTCTGGAGCATCCGCACGACTGCGGTGATATTACCGGAGACCTTCTGCGGGACGAGCCGGGTCACGC
GGCTGACGCGGAGCGTCCGTTGGGCGACAAACACCAGGACGGGGCACAGGTACACTATCTTGTCACCCGGAGGCGCGAGGGACTGCAGGAGCTT
CAGGGAGTGGCGCAGCTGCTTCATCCCCGTGGCCCGTTGCTCGCGTTTGCTGGCGGTGTCCCCGGAAGAAATATATTTGCATGTCTTTAGTTCT
ATGATGACACAAACCCCGCCCAGCGTCTTGTCATTGGCGAATTCGAACACGCAGATGCAGTCGGGGCGGCGCGGTCCCAGGTCCACTTCGCATA
TTAAGGTGACGCGTGTGGCCTCGAACACCGAGCGACCCTGCAGCGACCCGCTTAAAAGCTTGGCATTCCGGTACTGTTGGTAAAGCCACCATGG
CCGATGCTAAGAACATTAAGAAGGGCCCTGCTCCCTTCTACCCTCTGGAGGATGGCACCGCTGGCGAGCAGCTGCACAAGGCCATGAAGAGGTA
TGCCCTGGTGCCTGGCACCATTGCCTTCACCGATGCCCACATTGAGGTGGACATCACCTATGCCGAGTACTTCGAGATGTCTGTGCGCCTGGCC
GAGGCCATGAAGAGGTACGGCCTGAACACCAACCACCGCATCGTGGTGTGCTCTGAGAACTCTCTGCAGTTCTTCATGCCAGTGCTGGGCGCCC
TGTTCATCGGAGTGGCCGTGGCCCCTGCTAACGACATTTACAACGAGCGCGAGCTGCTGAACAGCATGGGCATTTCTCAGCCTACCGTGGTGTT
CGTGTCTAAGAAGGGCCTGCAGAAGATCCTGAACGTGCAGAAGAAGCTGCCTATCATCCAGAAGATCATCATCATGGACTCTAAGACCGACTAC
CAGGGCTTCCAGAGCATGTACACATTCGTGACATCTCATCTGCCTCCTGGCTTCAACGAGTACGACTTCGTGCCAGAGTCTTTCGACAGGGACA
AAACCATTGCCCTGATCATGAACAGCTCTGGGTCTACCGGCCTGCCTAAGGGCGTGGCCCTGCCTCATCGCACCGCCTGTGTGCGCTTCTCTCA
CGCCCGCGACCCTATTTTCGGCAACCAGATCATCCCCGACACCGCTATTCTGAGCGTGGTGCCATTCCACCACGGCTTCGGCATGTTCACCACC
CTGGGCTACCTGATTTGCGGCTTTCGGGTGGTGCTGATGTACCGCTTCGAGGAGGAGCTGTTCCTGCGCAGCCTGCAAGACTACAAAATTCAGT
CTGCCCTGCTGGTGCCAACCCTGTTCAGCTTCTTCGCTAAGAGCACCCTGATCGACAAGTACGACCTGTCTAACCTGCACGAGATTGCCTCTGG
CGGCGCCCCACTGTCTAAGGAGGTGGGCGAAGCCGTGGCCAAGCGCTTTCATCTGCCAGGCATCCGCCAGGGCTACGGCCTGACCGAGACAACC
AGCGCCATTCTGATTACCCCAGAGGGCGACGACAAGCCTGGCGCCGTGGGCAAGGTGGTGCCATTCTTCGAGGCCAAGGTGGTGGACCTGGACA
CCGGCAAGACCCTGGGAGTGAACCAGCGCGGCGAGCTGTGTGTGCGCGGCCCTATGATTATGTCCGGCTACGTGAATAACCCTGAGGCCACAAA
CGCCCTGATCGACAAGGACGGCTGGCTGCACTCTGGCGACATTGCCTACTGGGACGAGGACGAGCACTTCTTCATCGTGGACCGCCTGAAGTCT
CTGATCAAGTACAAGGGCTACCAGGTGGCCCCAGCCGAGCTGGAGTCTATCCTGCTGCAGCACCCTAACATTTTCGACGCCGGAGTGGCCGGCC
TGCCCGACGACGATGCCGGCGAGCTGCCTGCCGCCGTCGTCGTGCTGGAACACGGCAAGACCATGACCGAGAAGGAGATCGTGGACTATGTGGC
CAGCCAGGTGACAACCGCCAAGAAGCTGCGCGGCGGAGTGGTGTTCGTGGACGAGGTGCCCAAGGGCCTGACCGGCAAGCTGGACGCCCGCAAG
ATCCGCGAGATCCTGATCAAGGCTAAGAAAGGCGGCAAGATCGCCGTGTAATAATTCTAGAGTCGGGGCGGCCGGCCGCTTCGAGCAGACATGA
TAAGATACATTGATGAGTTTGGACAAACCACAACTAGAATGCAGTGAAAAAAATGCTTTATTTGTGAAATTTGTGATGCTATTGCTTTATTTGT
AACCATTATAAGCTGCAATAAACAAGTTAACAACAACAATTGCATTCATTTTATGTTTCAGGTTCAGGGGGAGGTGTGGGAGGTTTTTTAAAGC
AAGTAAAACCTCTACAAATGTGGTAAAATCGATAAGGATCCAGGTGGCACTTTTCGGGGAAATGTGCGCGGAACCCCTATTTGTTTATTTTTCT
AAATACATTCAAATATGTATCCGCTCATGAGACAATAACCCTGATAAATGCTTCAATAATATTGAAAAAGGAAGAGTATGAGTATTCAACATTT
CCGTGTCGCCCTTATTCCCTTTTTTGCGGCATTTTGCCTTCCTGTTTTTGCTCACCCAGAAACGCTGGTGAAAGTAAAAGATGCTGAAGATCAG
TTGGGTGCACGAGTGGGTTACATCGAACTGGATCTCAACAGCGGTAAGATCCTTGAGAGTTTTCGCCCCGAAGAACGTTTTCCAATGATGAGCA
CTTTTAAAGTTCTGCTATGTGGCGCGGTATTATCCCGTATTGACGCCGGGCAAGAGCAACTCGGTCGCCGCATACACTATTCTCAGAATGACTT
GGTTGAGTACTCACCAGTCACAGAAAAGCATCTTACGGATGGCATGACAGTAAGAGAATTATGCAGTGCTGCCATAACCATGAGTGATAACACT
GCGGCCAACTTACTTCTGACAACGATCGGAGGACCGAAGGAGCTAACCGCTTTTTTGCACAACATGGGGGATCATGTAACTCGCCTTGATCGTT

GGGAACCGGAGCTGAATGAAGCCATACCAAACGACGAGCGTGACACCACGATGCCTGTAGCAATGGCAACAACGTTGCGCAAACTATTAACTGG
CGAACTACTTACTCTAGCTTCCCGGCAACAATTAATAGACTGGATGGAGGCGGATAAAGTTGCAGGACCACTTCTGCGCTCGGCCCTTCCGGCT
GGCTGGTTTATTGCTGATAAATCTGGAGCCGGTGAGCGTGGGTCTCGCGGTATCATTGCAGCACTGGGGCCAGATGGTAAGCCCTCCCGTATCG
TAGTTATCTACACGACGGGGAGTCAGGCAACTATGGATGAACGAAATAGACAGATCGCTGAGATAGGTGCCTCACTGATTAAGCATTGGTAACT
GTCAGACCAAGTTTACTCATATATACTTTAGATTGATTTAAAACTTCATTTTTAATTTAAAAGGATCTAGGTGAAGATCCTTTTTGATAATCTC
ATGACCAAAATCCCTTAACGTGAGTTTTCGTTCCACTGAGCGTCAGACCCCGTAGAAAAGATCAAAGGATCTTCTTGAGATCCTTTTTTTCTGC
GCGTAATCTGCTGCTTGCAAACAAAAAAACCACCGCTACCAGCGGTGGTTTGTTTGCCGGATCAAGAGCTACCAACTCTTTTTCCGAAGGTAAC
TGGCTTCAGCAGAGCGCAGATACCAAATACTGTTCTTCTAGTGTAGCCGTAGTTAGGCCACCACTTCAAGAACTCTGTAGCACCGCCTACATAC
CTCGCTCTGCTAATCCTGTTACCAGTGGCTGCTGCCAGTGGCGATAAGTCGTGTCTTACCGGGTTGGACTCAAGACGATAGTTACCGGATAAGG
CGCAGCGGTCGGGCTGAACGGGGGGTTCGTGCACACAGCCCAGCTTGGAGCGAACGACCTACACCGAACTGAGATACCTACAGCGTGAGCTATG
AGAAAGCGCCACGCTTCCCGAAGGGAGAAAGGCGGACAGGTATCCGGTAAGCGGCAGGGTCGGAACAGGAGAGCGCACGAGGGAGCTTCCAGGG
GGAAACGCCTGGTATCTTTATAGTCCTGTCGGGTTTCGCCACCTCTGACTTGAGCGTCGATTTTTGTGATGCTCGTCAGGGGGGCGGAGCCTAT
GGAAAAACGCCAGCAACGCGGCCTTTTTACGGTTCCTGGCCTTTTGCTGGCCTTTTGCTCACATGGCTCGAC

8.5 Vector map: psiCheck2 – Promega

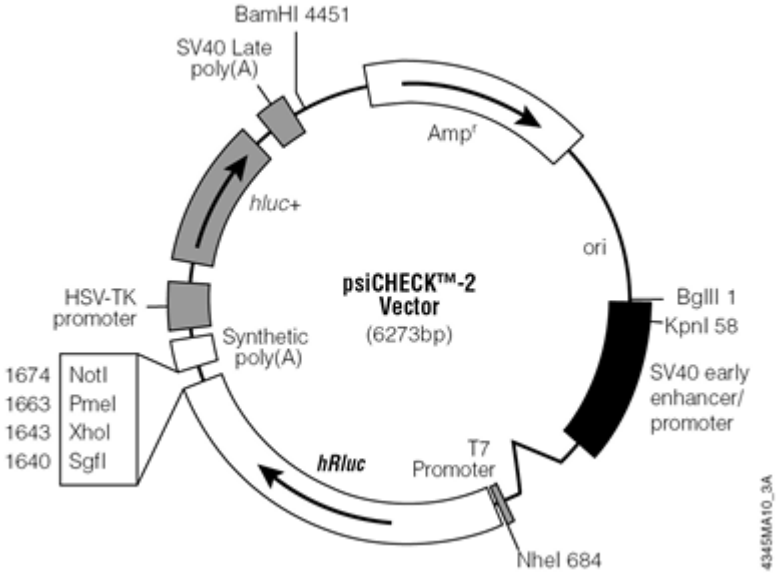

Figure 50: Vectormap of psiCheck2, Promega TB329, p10

8.6 List of abbreviations

53BP1	P53 binding protein 1
A	Adenosine
ALT	Alternative lengthening of telomeres
AMP	Adenosin monophosphate
Amp	Ampiciline
AP-1	Activator protein 1
ATM	ataxia-telangiectasia mutated
ATR	ataxia telangiectasia and Rad3 related
ATRA	All trans retinoid acid
BrdU	Bromodeoxyuridine
C. elegans	*Caenorhabditis elegans*
cDNA	Complementary DNA
CIP	Calf intestine phosphatase
Ct	Cycle threshold value
Ctrl	Control
D. melanogaster	*Drosophila melanogaster*
DDR	DNA damage response
DGCR8	DiGeorge syndrome critical region gene 8
DNA	Desoxiribonucleic acid
DROSHA	drosha, ribonuclease type III
DSB	Double strand break
E. coli	*Escherichia coli*
EtOH	Ethanol
FACS	Fluorescence activated cell sorting
FAM	Famylation
FFluc	Firefly luciferase
FITC	Fluorescein isothiocyanate
GAPDH	glyceraldehyde-3-phosphate dehydrogenase
GFP	Green fluorescent protein
H_2O_2	Hydrogen peroxide
HDF	Human diploid fibroblasts
HeLa cells	Henrietta Lacks cervical cancer cells
IGF-1	Insulin like growth factor 1
JunB	jun B proto-oncogene
JunD	jun D proto-oncogene
MAPK	Mitogen activated protein kinase
MDC1	mediator of DNA-damage checkpoint 1
miR/miRNA	microRNA
mRNA	Messenger RNA
mut	mutant
NBS1	Nijmegen breakage syndrome protein 1
NFW	Nuclease free water
NPC	Nasopharyngeal carcinoma cell
ORF	Open reading frame
P	Phosphate
p.T.	Post transfection/treatment
p16 (CDKN2A)	p16 protein (cyclin-dependent kinase inhibitor 2A)
p21 (CDKN1A)	p21 protein (cyclin-dependent kinase inhibitor 1A)
p53	Tumor protein p53
PAA	Polyacrylamide
PAGE	Polyacrylamide gel electrophoresis
P-bodies	Processing bodies
PCR	Polymerase chain reaction
Pd	Population doublings
PI	Propidium Iodide

PP5	Protein phosphatase 5
psiC2	psiCheck2
PUVA	Psoralens and UV-A light
qPCR	Quantitative (Realtime) PCR
Rb	Retinoblastoma
RISC	RNA induced silencing complex
Rluc	*Renilla* luciferase
RNA	Ribonucleic acid
RNAi	RNA interference
ROS	Reactive oxygen species
rRNA	Ribosomal RNA
RS	Replicative senescence
SDS	Sodium dodecyl sulfate
SEM	Standard error of the mean
siRNA	Small interfering RNA
SOC	Super Optimal broth with catabolite repression
T	Thymidine
Taq	*Thermophilus aquaticus*
TGFb	transforming growth factor, beta
TOR	Target of rapamycin
UTR	Untranslated region
UV	Ultra violet
UV-A	Ultra violet-A light (380–315nm wavelength)

9 ZUSAMMENFASSUNG

Das Altern ist ein biologischer Prozess, den man von der Zelle bis zur Gesamtorganismus beobachten kann und der durch einen fortschreitenden Funktionsverlust gekennzeichnet ist welcher zu Krankheiten und letztlich zum Tod führt. Auf zellulärer Ebene sind die grundlegenden Mechanismen die zur Seneszenz führen, ein Schutz vor ungebremster Proliferation und damit Hindernis bei der Entstehung von Krebs. So fließen in die Regulation Informationen über DNA Integrität, reaktive Stoffwechselprodukte und den generellen Stressstatus der Zelle ein. Können die Schäden nicht repariert werden, so werden komplexe verflochtene Signalwege aktiviert, wodurch die Zelle in Apoptose oder finalen Wachstumsarrest geht.

Eine Ebene dieser Regulierung findet über microRNAs statt: kurze RNAs, welche über RNA Interferenz die Stabilität von mRNAs beeinflussen. Eine miRNA kann, weil dafür keine 100%ige Komplementarität notwendig ist, mehrere verschiedene mRNAs regulieren.

In einem Vorversuch wurde in hsa-miR-663 eine miRNA gefunden die in der zellulären Seneszenz von menschlichen Hautfibroblasten hoch reguliert ist und von der bioinformatisch bestimmt wurde, dass sie die Zellzyklusphosphatase PP5 binden könne. PP5 wirkt mit in der Regulation von vielen Signalewegen für die für die Seneszenz entscheidend sind und beeinflusst auch die Aktivität eines der wichtigsten zellulären Stress Mediatoren: p53. Unter anderem induziert p53 die Transkription von p21, der als Zellzyklus Inhibitor einen G1 arrest auslösen kann.

Dies direkte Interaktion zwischen miR-663 und PP5 wollten wir mithilfe eines Reporter-Gen-Vektors bestätigen: wir koppelten die 3‘ untranslatierte Region (3’UTR) von PP5 an eine Luciferase und wollten RNA Interferenz – ausgelöst durch die Bindung von miR-663 - über ein vermindertes Luciferase signal detektieren. In den durchgeführten Experimenten wurde jedoch kein eindeutiger Hinweis für eine direkte Interaktion zwischen miR-663 und der 3‘UTR gesehen. Als Folge von Überexprimierung von miR-663 sahen wir eine Reduktion an zellulärem PP5 Protein Gehalt, der sich auf mRNA Ebene nicht widerspiegelte und reduzierte Level an p21 mRNA. Einen Einfluss auf das Wachstumsverhalten von Zellen – ermittelt durch den Einbau von BrdU während der DNA Replikation – konnte weder in Zellen gesehen werden, die mit miR-663 transfeziert wurden, noch in solchen, deren PP5 mithilfe einer siRNA reduziert wurde. Die Behandlung von humanen Fibroblasten mit einer H2O2 um DNA Schäden zu induzieren führte zu einer Zunahme an p21 mRNA, welche jedoch nicht mit der Menge an PP5 mRNA oder dem Level an miR-663 korrelierte.

10 CURRICULUM VITAE

Kathrin Ingrid Garschall

Education

since 2003	Undergraduate studies: **Molecular Biology** at the **University of Vienna**
2006 – 2010	Undergraduate studies: **Food- and Biotechnology** At the **University of Natural Resources and Applied Life Sciences, Vienna (BOKU)**
May 2003	**Matura** (A-Levels) at Stiftsgymnasium Melk

Research and work experience

January 2011 - March 2012	**Practical training** with **Wolfgang J. Miller** (PI), Laboratories of Genome Dynamics, Medical University of Vienna Determination of *Wolbachia* prevalence in *Glossina spp.* by VNTR PCR and Southern Blot
October 2011 - December 2011	**Practical training** with **Franz Klein** (PI), Max F. Perutz Laboratories, Vienna: Recombineering of a plasmid to study hotspot/axis determination during meiotic recombination in yeast
January 2010 – May 2010; **June 2010– May 2011**	**Diploma thesis** with **Johannes Grillari** (PI), Institute of Applied Microbiology, University of Natural Resources and Applied Life Sciences, Vienna (BOKU) Study of human miR-663 in replicative cellular senescence
October 2008 - February 2010	**Laboratory tutor** for the Bachelor studies practical course "Molecular Biology" at University of Natural Resources and Applied Life Sciences, Vienna (BOKU)
September 2010	**Poster presentation** at the 2nd ÖGMBT annual meeting: "Impact of miR-663 on cell cycle phosphatase PP5 in cellular senescence"
May 2010	**Practical training** with **Timothy Skern** (PI), Max F. Perutz Laboratories, Vienna Cloning of HRV2 and PV Protease 2A to an expression vector for clarification of structure and self-release mechanism
October 2009 – January 2010	**Practical training** with **Johannes Grillari** (PI), Institute of Applied Microbiology, University of Natural Resources and Applied Life Sciences, Vienna (BOKU) Cloning of a reporter construct to determine miRNA-target interaction in human primary cells
August 2004	**Practical training** at the general laboratory, **Hospital SMZ Ost**, Vienna: Assistance to a clinical study on minimal residual disease (MRD) in blood and serum samples of colon tumor patients

Publications

Schneider DI, Garschall KI, Parker AG, Abd-Alla AM, Miller WJ. (2012)
"Global *Wolbachia* prevalence, titer Fluctuations and their potential of causing cytoplasmic incompatibilities in tsetse flies and hybrids of *Glossina morsitans* subgroup species." Journal of Invertebrate Pathology 2012 Apr 10. (in press)

Garschall KI, Wieser M, Kühnel H, Schosserer M, Grillari R and Grillari J (2010)
"Impact of miR-663 on cell cycle phosphatase PP5 in cellular senescence" - Poster for the ÖGMBT annual meeting 2010.

Vienna, February 20th 2013